Supporting Information for

Straightforward access to biocompatible poly(2-oxazoline)-coated nanomaterials by polymerization-induced self-assembly

Dao Le,[‡ab] Friederike Wagner,[‡ab] Masanari Takamiya,[a] I-Lun Hsiao,[ac] Gabriela Gil Alvaradejo,[ab] Uwe Strähle,[a] Carsten Weiss,[a] Guillaume Delaittre[ab]*

[a]Institute of Toxicology and Genetics (ITG), Karlsruhe Institute of Technology (KIT), Hermann-von-Helmholtz-Platz 1, 76344 Eggenstein-Leopoldshafen, Germany.
[b]Institute for Chemical Technology and Polymer Chemistry (ITCP), Karlsruhe Institute of Technology (KIT), Engesserstr. 18, 76128 Karlsruhe, Germany.
[c]School of Food Safety, College of Nutrition, Taipei Medical University, No.250, Wuxing St., Taipei 11031, Taiwan.
[‡]These authors contributed equally.
Email: guillaume.delaittre@kit.edu

Table of contents

Materials

2-Hydroxypropyl methacrylate (HPMA; Alfa Aesar, 98 %) and benzyl methacrylate (BzMA; Sigma-Aldrich, 96 %) were passed through a basic aluminum oxide column to remove inhibitor prior to polymerization. 2-Ethyl-2-oxazoline (EtOx; Acros Organics, > 99 %) and methyl *p*-toluenesulfonate (MeOTs; Sigma-Aldrich, 98 %) were purified by vacuum distillation. Azobisisobutyronitrile (AIBN; Sigma-Aldrich, 98 %) was recrystallized from ethanol. 4-Cyano-4-(phenylcarbonothioylthio)pentanoic acid (ACPDB; Sigma-Aldrich, 97 %), triethylamine (TEA; Fisher Scientific), acetonitrile (MeCN; Acros Organics), diethyl ether (Et_2O; Carl Roth), propargyl alcohol (Alfa Aesar, 99 %), 1-ethyl-3-(3-dimethylaminopropyl) carbodiimide hydrochloride (EDC-HCl; Carl Roth, ≥ 99 %), 4-(dimethylamino)pyridine (DMAP; Sigma Aldrich, ≥ 99 %), sodium azide (Carl Roth, ≥ 99 %), 1,1,4,7,7-pentamethyldiethylenetriamine (PMDETA; Acros Organics, 98 %+), copper(I) bromide (Sigma-Aldrich, 99.999 %), ethylenediaminetetraacetic acid disodium salt dihydrate (EDTA-Na_2; Carl Roth, ≥ 99%) and fluorescein *O*-methacrylate (FMA; Sigma-Aldrich, 97 %) were used without any further purification. 100-nm FITC-labeled carboxylated polystyrene nanoparticles (PS-COOH NPs) were purchased from Polysciences, Inc., PA, USA. Sodium phenyl-2,4,6-trimethylbenzoylphosphinate (SPTP)[1] and tetraethylrhodamine 4-vinylbenzyl ester (RVB)[2] were synthesized according to reported procedures.

Characterization methods

Nuclear magnetic resonance (NMR) spectroscopy

^{1}H NMR spectroscopy was performed on a Bruker NMR 500 spectrometer at 500 MHz. The samples were dissolved in deuterated solvent. The solvent signals were employed for chemical shift corrections.

Size-exclusion chromatography (SEC) in DMAc

Size-exclusion chromatography was performed on a Polymer Laboratories PL-SEC 50 Plus Integrated System comprising an autosampler, a PLgel 2.5 µm bead-size guard column (50 × 7.5 mm), followed by three PLgel 5 µm Mixed-C columns (300 × 7.5 mm), and a differential refractive index detector. *N,N*-Dimethylacetamide (DMAc) was employed as solvent with a flow rate of 1 mL min^{-1} and a sample concentration of 2 g L^{-1}. The SEC system was calibrated with linear poly(methyl methacrylate) (PMMA) standards ranging from 700 to 2 × 10^6 g mol^{-1}. Prior to injection samples were filtered through PTFE membranes with a pore size of 0.2 µm.

SEC in THF

Measurements were performed on a TOSOH Eco-SEC HLC-8320 GPC system, which comprised an autosampler, a SDV 5 µm bead size guard column (50 × 8 mm, PSS) followed by three SDV 5 µm columns (300 × 7.5 mm, subsequently 100, 1000, and 10^5 Å pore size, PSS), a differential refractive index (DRI) detector, and UV-Vis detector set to 320 nm, with THF as the eluent at 30 °C with a flow rate of 1 mL min^{-1}. The SEC system was calibrated by using, with linear PMMA standards ranging from 800 to 1.82 × 10^6 g mol^{-1}. Calculation of the molar mass proceeded by using a relative calibration based on PMMA standards.

Dynamic light scattering (DLS)

DLS measurements were performed at 25 °C at an angle of 173° (backscattering mode) with a Zetasizer Nano S from Malvern using a 4mW He-Ne laser at 633 nm. Analysis of the data was carried out using the Nano DTS v.5.10 software. Nanoparticles obtained from PISA were diluted in water to a concentration of 1 mg mL^{-1} and were not filtered prior to the measurements. Experiments were performed with 12 readouts of 3 independent measurements for each sample.

Transmission electron microscopy (TEM)

TEM observations were carried out on a Zeiss EM 109T instrument operated at 80 kV. The polymerization reaction mixtures were diluted in water to a concentration of 1 mg mL^{-1}. 10 µL of uranyl acetate solution (1 wt%) were then mixed with 1 mL of this particle solution. A drop of 6 µL of the solution was placed on a copper grid for 20 seconds and then blotted using filter paper to remove excess solution.

For the samples at 4, 15, and 40 °C: All materials and solutions were kept at the corresponding predetermined temperature for 60 minutes prior to the preparation.

SEC-ESI-MS

Electrospray ionization mass spectrometry (ESI-MS) measurements were performed on a Q-Exactive Orbitrap mass spectrometer (Thermo Fisher Scientific, San Jose, CA, USA) with SEC hyphenation. The instrument was calibrated in the 195–1822 *m*/*z* range using calibration solutions from Thermo Fisher Scientific. The samples were prepared by dissolving in THF at a concentration of 2 mg mL^{-1}.

UV-Vis spectroscopy

UV-Vis measurements were performed on a Lambda 35 UV-Vis spectrometer (Perkin Elmer, US) in a quartz cuvette. The spectra were recorded in water or DCM at 25 °C between 200 and 700 nm with a sample concentration of 0.05 mg mL^{-1}.

Fluorescence spectroscopy

Fluorescence measurements were carried out on a Varian Cary Eclipse spectrometer with an excitation slit width of 5 nm, a resolution of 0.5 nm, and a scan rate of 30 nm min^{-1} in water at 25 °C. The excitation wavelength for FMA and RVB are 490 and 555 nm, respectively. The analytes were dissolved in water with a concentration of 0.1 mg mL^{-1}.

Synthesis

Alkynyl-functionalized RAFT agent

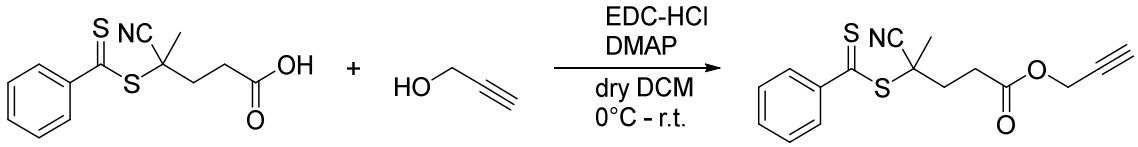

ACPDB (1.0 g, 3.58 mmol, 1.0 eq.), propargyl alcohol (461.4 mg, 8.23 mmol, 2.3 eq.), and DMAP (87.5 mg, 0.716 mmol, 0.2 eq.) were dissolved in 15 mL anhydrous DCM. The red solution was cooled to 0 °C and 1-ethyl-3-(3-dimethylaminopropyl)carbodiimide (EDC-HCl, 1.373 g, 7.16 mmol, 2.0 eq.) in 5 mL anhydrous DCM was added. After 1 h, the reaction mixture was warmed to room temperature and stirred for 18 h. The reaction mixture was washed four times with 0.1 M HCl solution and twice with water. The organic phase was dried over sodium sulfate and filtered. The solvent was then evaporated under reduced pressure. The product was purified by column chromatography using cyclohexane/ethyl acetate 4:1 v/v as eluent. The alkynyl RAFT agent was obtained as a red oil (0.699 g, 62 %).

^{1}H NMR ($CDCl_3$, 500 MHz): δ / ppm = 7.90 (d, 2H), 7.55 (t, 1H), 7.40 (t, 2H), 4.72 (s, 2H), 2.78 - 2.43 (m, 5H), 1.94 (s, 3H).

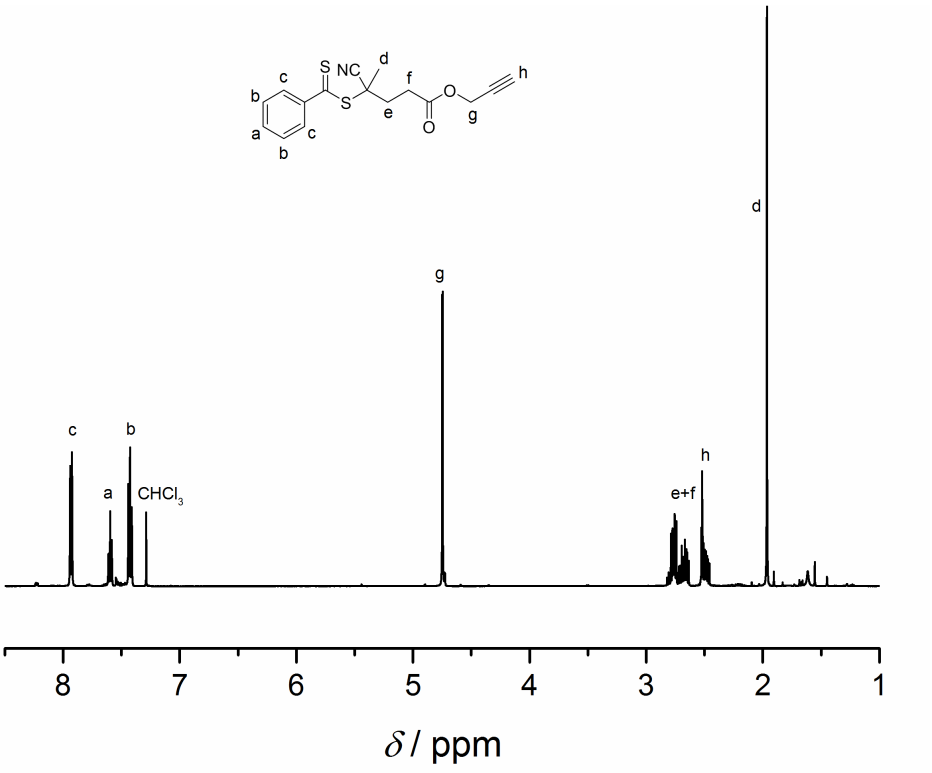

Figure S1. ^{1}H NMR spectrum of alkynyl-functionalized RAFT agent; solvent: $CDCl_3$.

Kinetic of CROP of 2-ethyl-2-oxazoline with termination by carboxylic RAFT agent or sodium azide

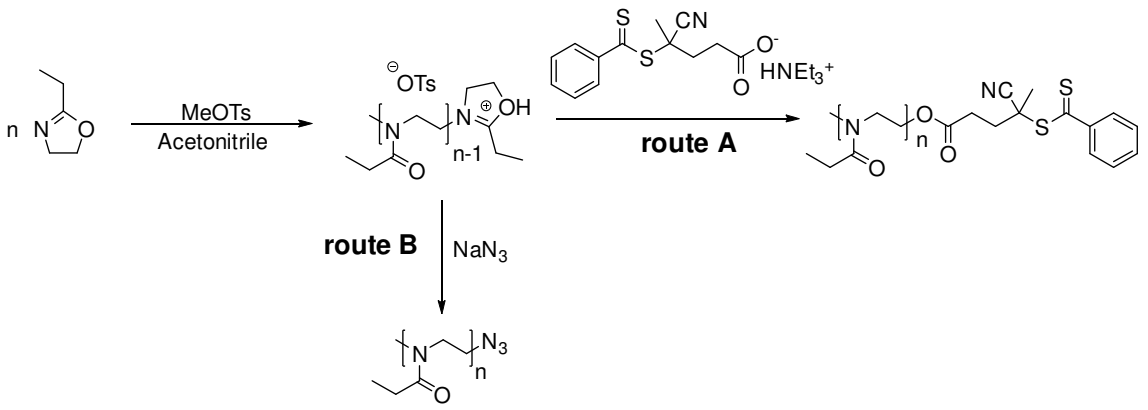

For each kinetic run, a mixture of EtOx (1.3 mL, 113 eq.) and MeOTs (24.6 mg, 1 eq.) in 1.9 mL MeCN was added in 4 vials. Polymerization was conducted by heating at 82 °C. After 1, 2, 4, and 6 hours, polymerization was quenched by adding either 3 eq. of sodium azide or a mixture of 1.5 eq. of ACPDB and 3 eq. of TEA. The monomer conversion was determined by ^{1}H NMR spectroscopy. The molar mass distributions were monitored by SEC in DMAc without purification.

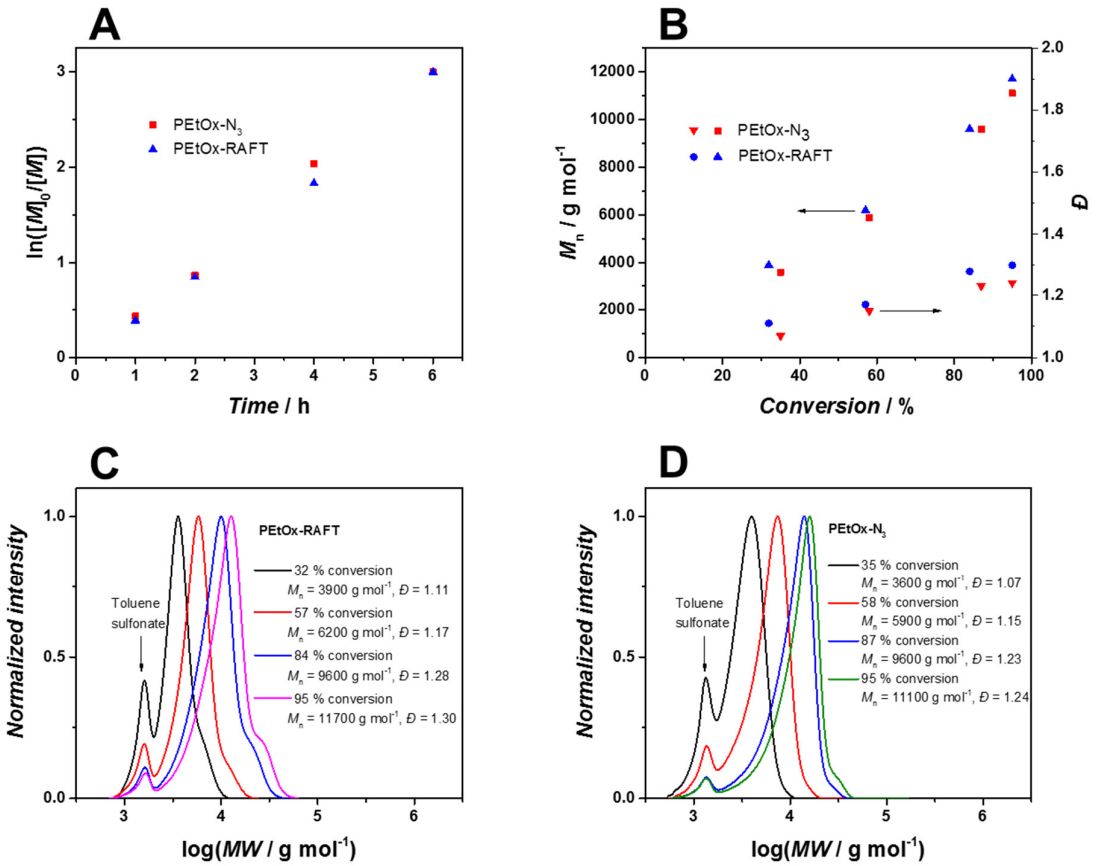

Figure S2. (A) Pseudo first-order kinetic plot and (B–D) SEC data in DMAc for the CROP of EtOx initiated by methyl tosylate in acetonitrile at 82 °C with [EtOx]/[MeOTs] = 113 and terminated by carboxylic RAFT agent or sodium azide.

PEtOx-CTA synthesis by direct termination

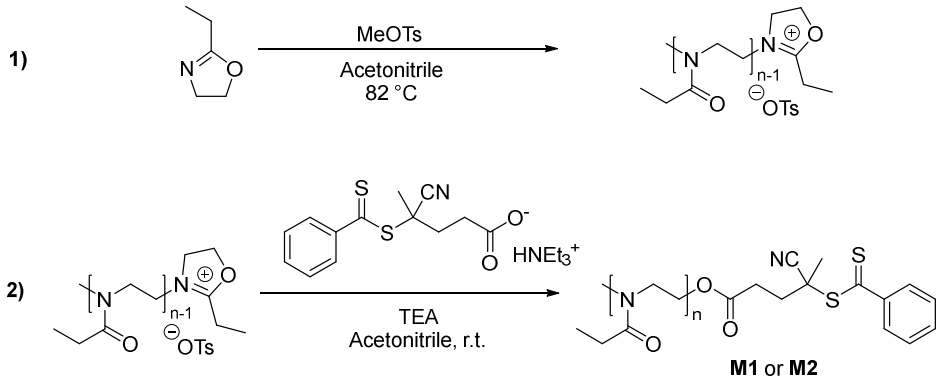

In a glove box, anhydrous MeCN (14.4 mL), MeOTs (185 mg, 0.99 mmol, 1 eq.), and EtOx (10.0 mL, 115 mmol, 116 eq.) were added in a flask. The flask was closed air-tight with a septum. The polymerization was carried out in an oil bath at 82 °C for 2 h or 4 h for **M1** and **M2**, respectively, depending on the targeted molar mass of the final polymer. The reaction was cooled to room temperature and quenched by adding ACPDB (415 mg, 1.5 mmol, 1.5 eq.) and TEA (300 µL, 3.0 mmol, 3 eq.) in 2 mL anhydrous MeCN. The mixture was stirred at room temperature overnight. The solution was concentrated under reduced pressure and passed twice through a basic Al_2O_3 column. The polymer was precipitated into cold Et_2O and obtained as a pink powder after drying under vacuum.

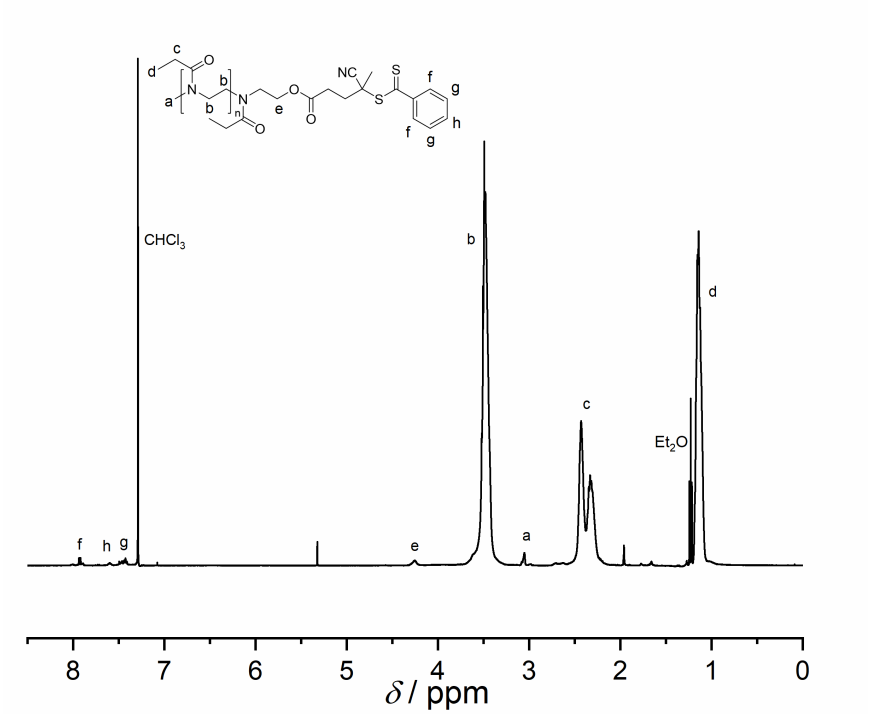

Figure S3. ^{1}H NMR spectrum of PEtOx-CTA **M1**; solvent: $CDCl_3$.

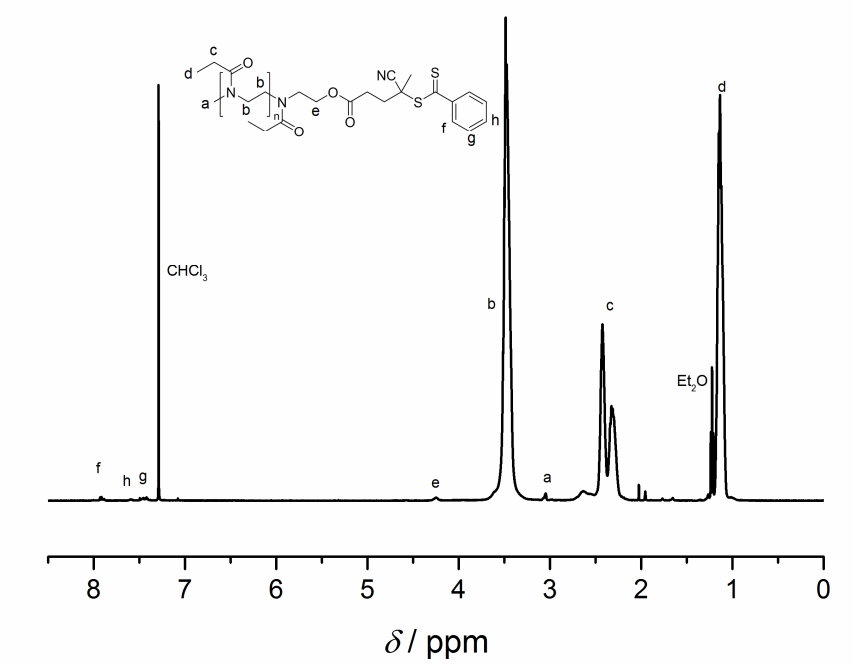

Figure S4. ^{1}H NMR spectrum of PEtOx-CTA **M2**; solvent: $CDCl_3$.

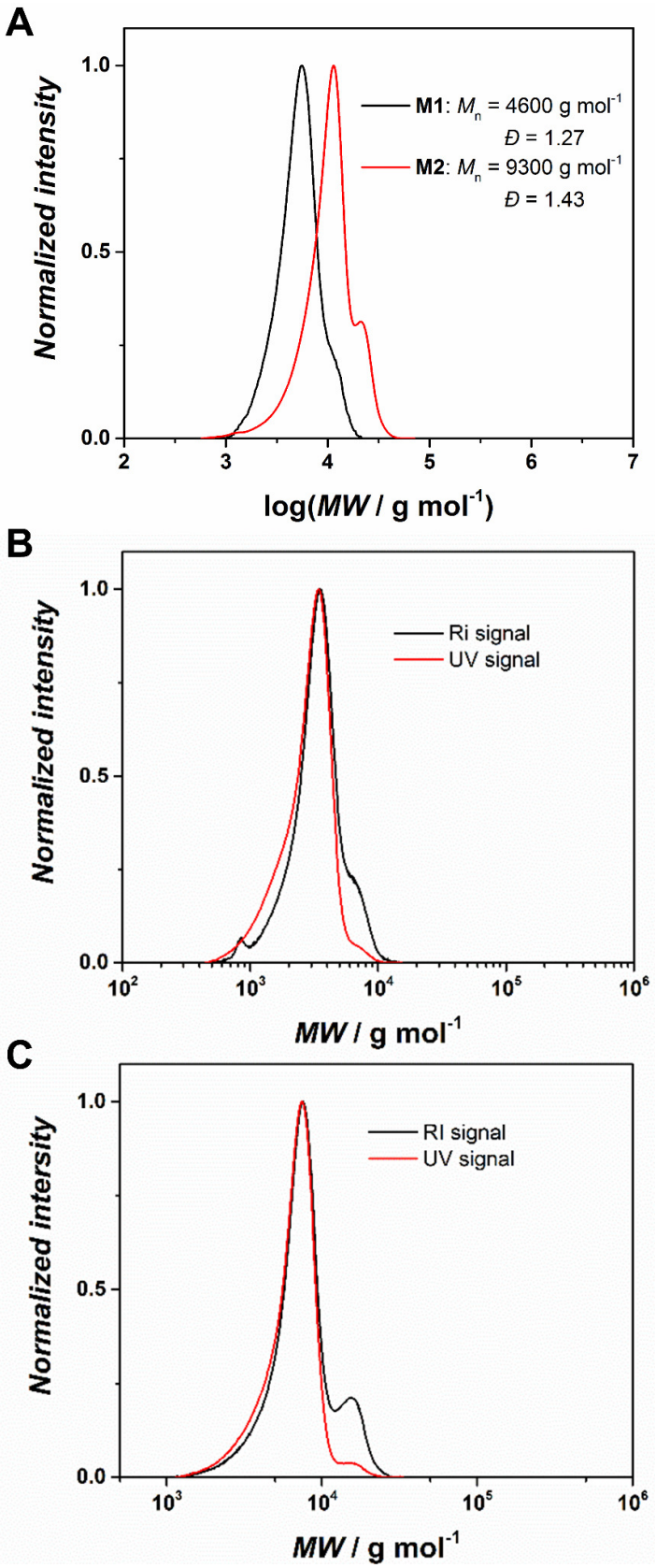

Figure S5. Size-exclusion chromatograms of (A) **M1** and **M2** in DMAc, (B) **M1** in THF, and (C) **M2** in THF. *Note the relatively low UV intensity for the high molar mass shoulder, indicative of chains not bearing the RAFT moiety.*

Azide-terminated PEtOx synthesis

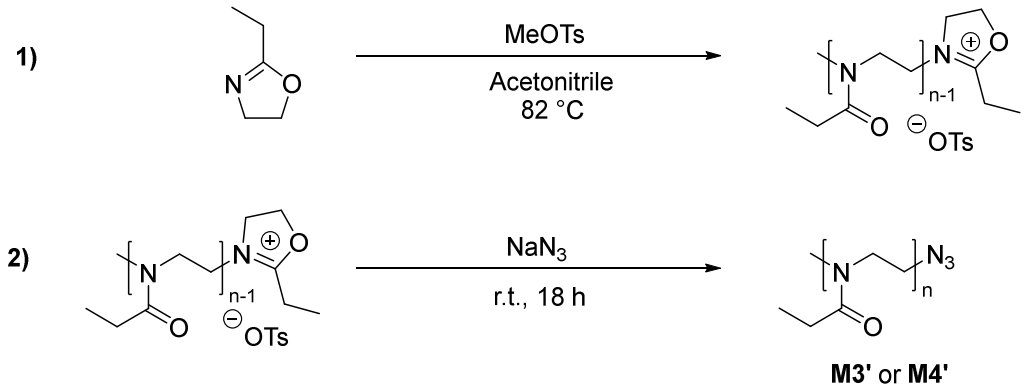

In a glove box, anhydrous MeCN (14.4 mL), MeOTs (185 mg, 0.99 mmol, 1 eq.), and EtOx (10.0 mL, 115 mmol, 116 eq.) were added in a flask. The flask was closed air-tight with a septum. The polymerization was carried out in an oil bath at 82 °C for 2 h or 4 h for **M3'** and **M4'**, respectively, depending on the targeted molar mass of the final polymer. The reaction was cooled to room temperature and quenched by adding an excess of sodium azide (322 mg, 4.95 mmol, 5 eq.) under a nitrogen atmosphere. The mixture was stirred at ambient temperature overnight. The solution was diluted with DCM and washed three times with brine. The organic phase was dried over sodium sulfate and filtered. The solvent was removed under reduced pressure. The crude product was dissolved in a small amount of DCM. The polymer was precipitated into cold Et_2O and obtained as a white powder after drying under vacuum.

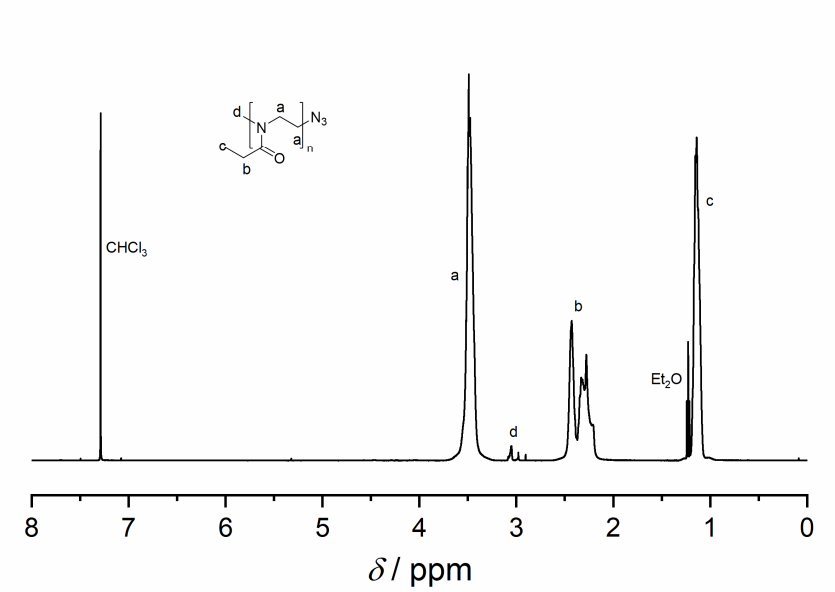

Figure S6. ^{1}H NMR spectrum of PEtOx-N_3 **M3'**; solvent: $CDCl_3$.

PEtOx-CTA synthesis via click reaction

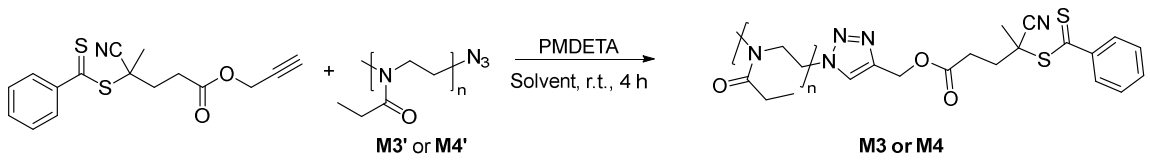

Azide-terminated poly(2-ethyl-2-oxazoline) PEtOx-N_3 (0.51 mmol, 1.0 eq.) and alkynyl-functionalized RAFT agent (194.3 mg, 0.61 mmol, 1.2 eq.), copper(I) bromide (22.0 mg, 0.153 mmol, 0.3 eq.), and 25 mL DCM were added in 50 mL round bottom flask. The reaction mixture was deoxygenated by nitrogen bubbling for 30 minutes. In another round bottom flask, PMDETA (160 µL, 0.765 mmol, 1.5 eq.) was diluted in 2 mL dry DCM. This solution was deoxygenated by nitrogen bubbling for 30 min and subsequently transferred to the flask containing the former mixture of PEtOx-N_3, RAFT agent, and CuBr using a deoxygenated syringe. The reaction was stirred at room temperature for 4 h. The solution was diluted with 20 mL DCM and washed three times with 10 mL of an aqueous EDTA-Na_2 solution (1 wt%). The organic phase was dried over sodium sulfate. The solvent was evaporated under reduced pressure. The crude product was dissolved in a small amount of DCM. The RAFT-functionalized PEtOx was precipitated twice into cold Et_2O and obtained as a pink powder.

^{1}H NMR ($CDCl_3$, 500 MHz): δ/ppm = 7.88 (d, 2H), 7.65 (t, 1H), 7.57 (t, 1H), 7.40 (t, 2H), 5.23 (s, 2H), 4.60 (s, 2H), 3.84 (s, 2H), 3.47 (s, 4H), 3.03 (s, 3H), 2.40 - 2.29 (m, 2H), 1.11 (s, 3H).

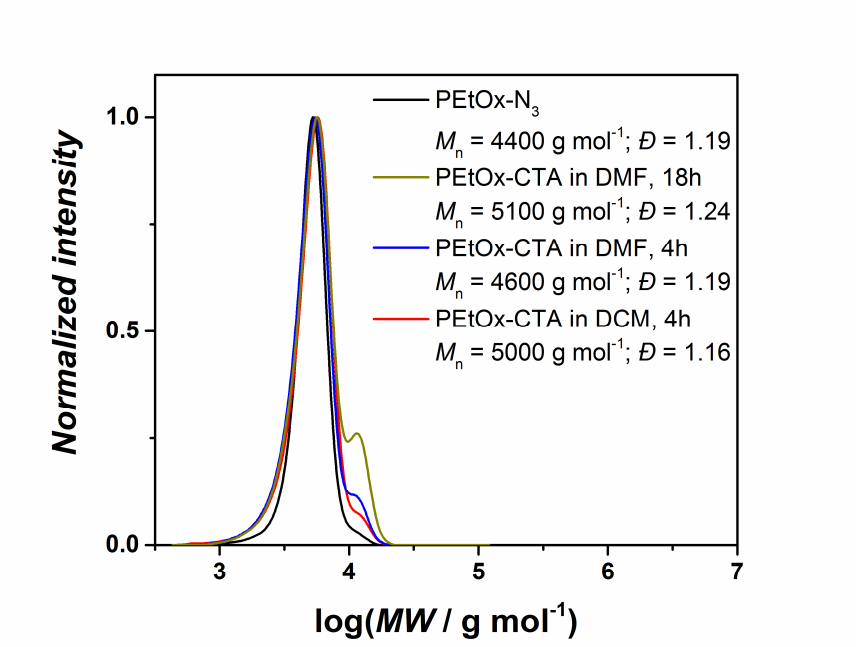

Figure S7. Size-exclusion chromatograms in DMAc of PEtOx-N_3 before and after click reaction with an alkynyl-functionalized CTA in different solvents and for varying reaction times.

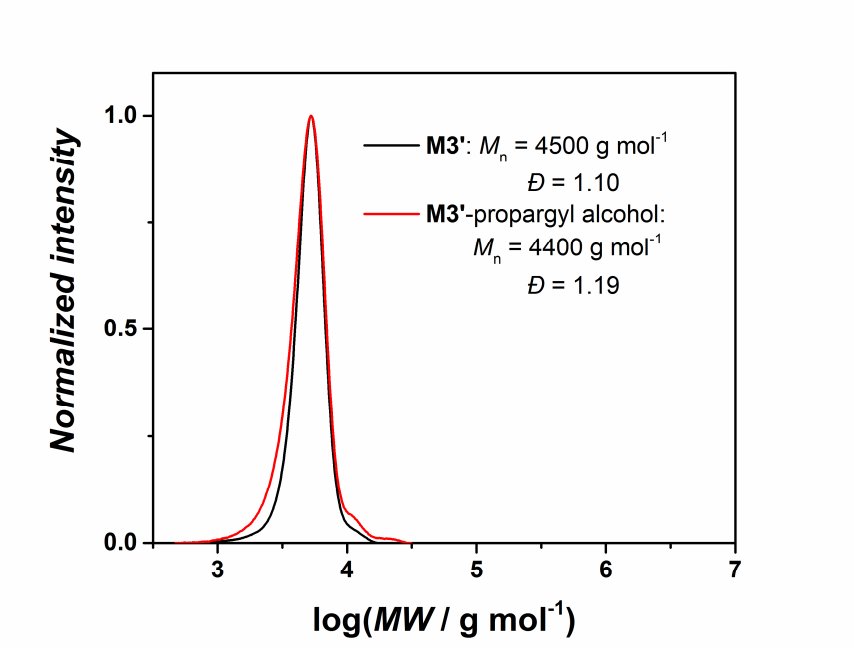

Figure S8. Size-exclusion chromatograms in DMAc of **M3'** and of the product of its modification by CuAAC with propargyl alcohol.

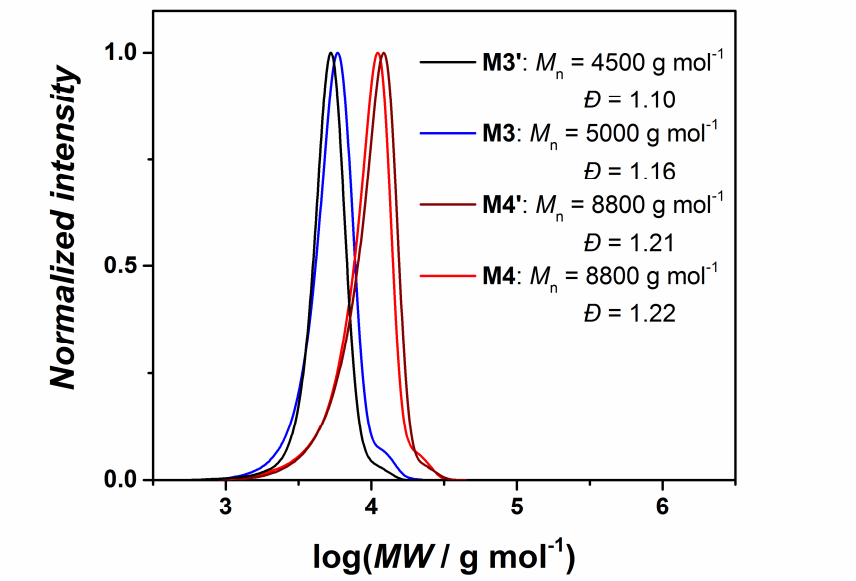

Figure S9. Size-exclusion chromatograms in DMAc of **M3** and **M4** and their azide-functionalized precursors **M3'** and **M4'**, respectively.

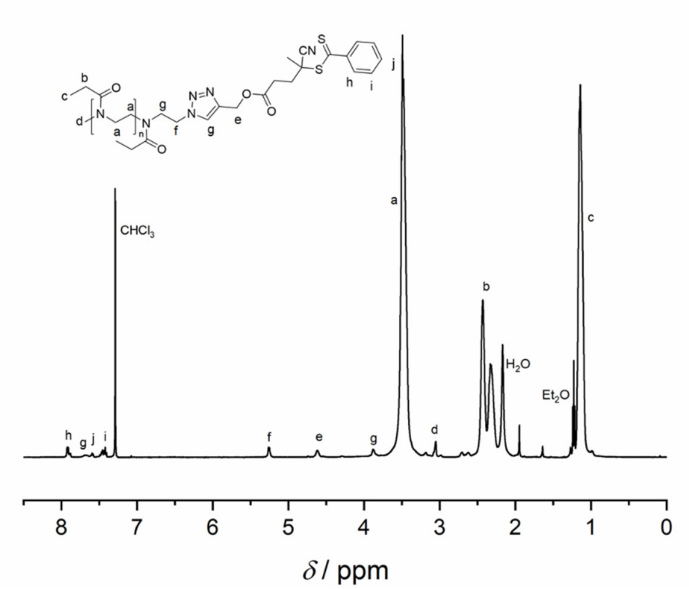

Figure S10. ^{1}H NMR spectrum of PEtOx macroRAFT agent **M3**; solvent: $CDCl_3$.

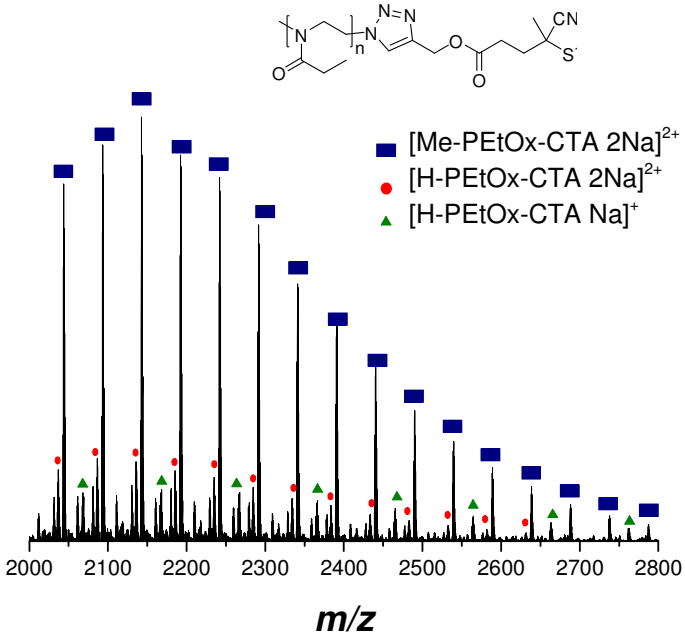

Figure S11. Mass spectrum of PEtOx-CTA **M3**. *We note that close to all detected species possess the desired RAFT end group.*

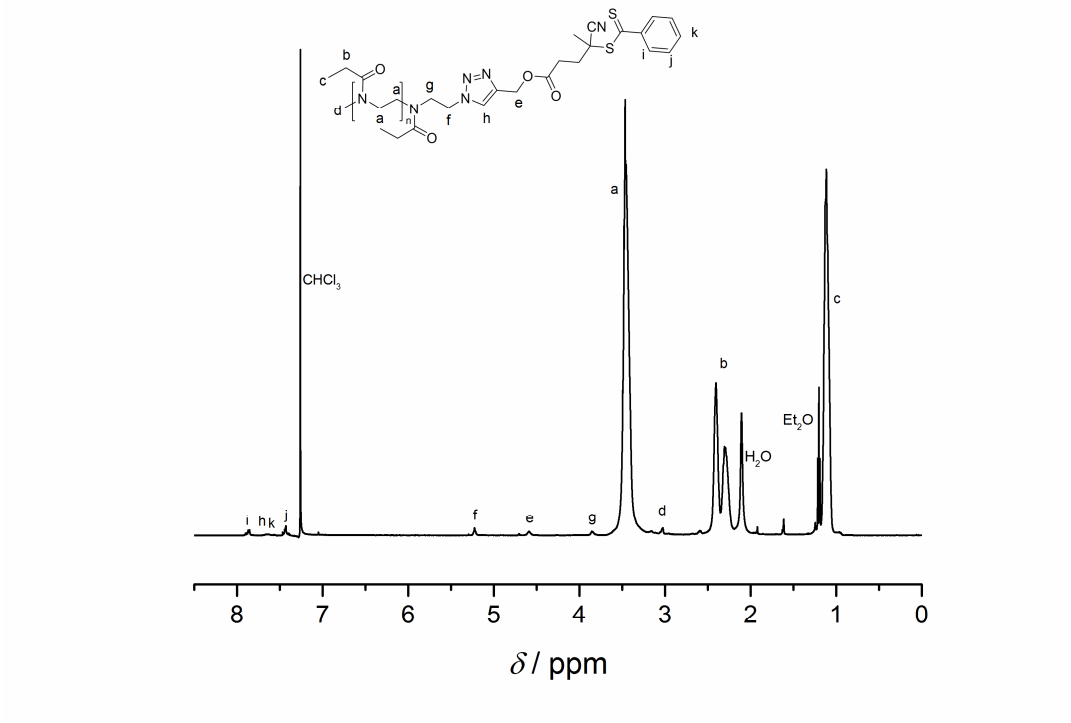

Figure S12. ^{1}H NMR spectrum of PEtOx macroRAFT agent **M4**; solvent: $CDCl_3$.

Table S1. Characterization of PEtOx-CTA used in this study.

PEtOx-CTA	$M_{n,NMR}$ / g mol^{-1}	$M_{n,SEC}$ / g mol^{-1}	$Đ_{SEC}$
M1[a]	5500	4600	1.27
M2[a]	9200	9300	1.43
M3[b]	5300	5000	1.16
M4[b]	9500	8800	1.22

[a]Obtained by direct termination with deprotonated ACPDB (Route A).

[b]Obtained by termination with NaN_3 and CuAAC with alkyne-RAFT agent (Route B).

Chain extension in solution

MacroCTA (1 eq.), BzMA (100 or 150 eq.), and AIBN (0.2 eq.) in dry MeCN were added to a headspace vial. The vial was closed air-tight and deoxygenated by nitrogen bubbling for 20 min. The reaction mixture was heated in an oil bath at 70 °C for 24 h, after which the reaction mixture was cooled to room temperature. The conversion was determined by ^{1}H NMR spectroscopy on the reaction mixture. The molar mass of the dried raw product was determined by SEC in DMAc.

Table S2. Experimental conditions and results for the chain extension of macroCTAs in solution.

macroCTA	BzMA	AIBN	MeCN	*Conversion*[a] *%*	$M_{n,SEC}$[b] *g mol^{-1}*	*Đ*[b]
M2 100 mg 0.011 mmol 1 eq.	294 mg 1.667 mmol 150 eq	0.365 mg 0.002 mmol 0.2 eq.	0.4 mL	90	24200	1.43
M3 50 mg 0.011 mmol 1 eq.	200 mg 1.136 mmol 100 eq.	0.373 mg 0.002 mmol 0.2 eq.	0.4 mL	82	15200	1.28
M4 50 mg 0.006 mmol 1 eq.	160 mg 0.910 mmol 100 eq.	0.199 mg 0.001 mmol 0.2 eq.	0.4 mL	82	16900	1.30

Determined by [a]1H NMR spectroscopy and [b]size-exclusion chromatography.

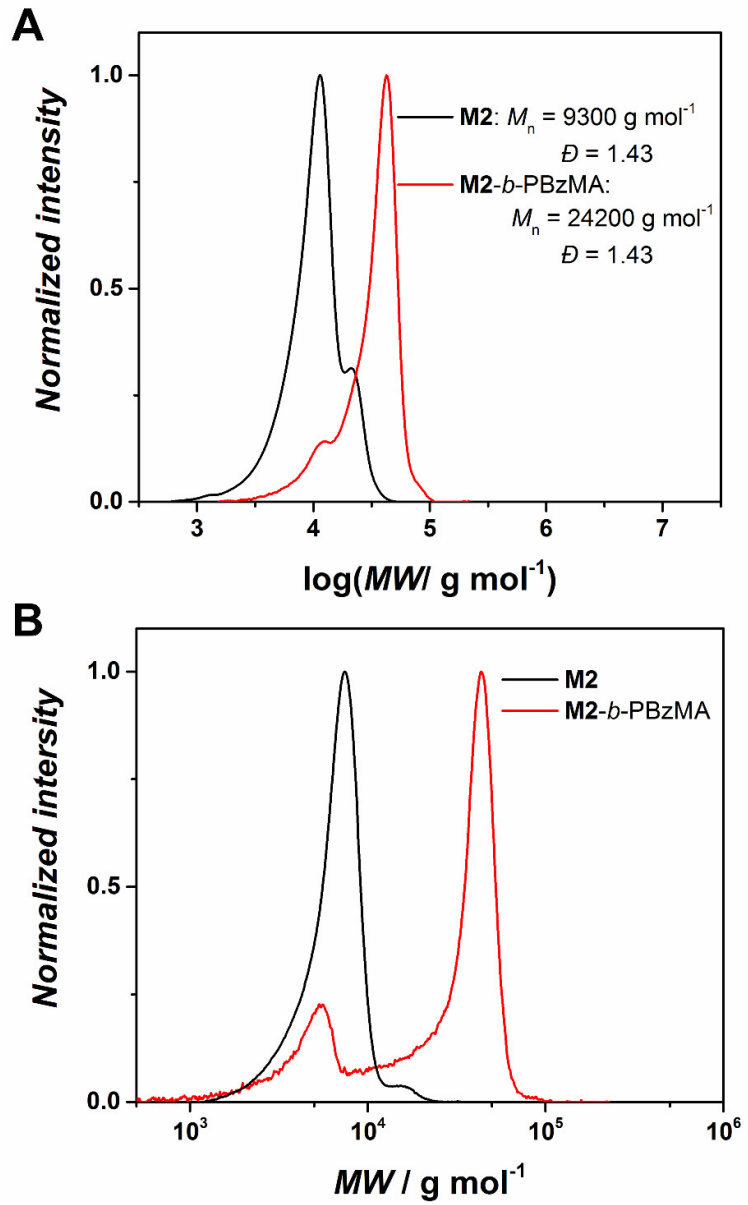

Figure S13. Size-exclusion chromatograms of **M2** and of its chain extension product with benzyl methacrylate in DMAc with RI detection (A) and in SEC with UV detection at 320 nm (B). *We note the presence of a non-negligible fraction of PEtOx chains that seem to carry the RAFT moiety but were not chain-extended.*

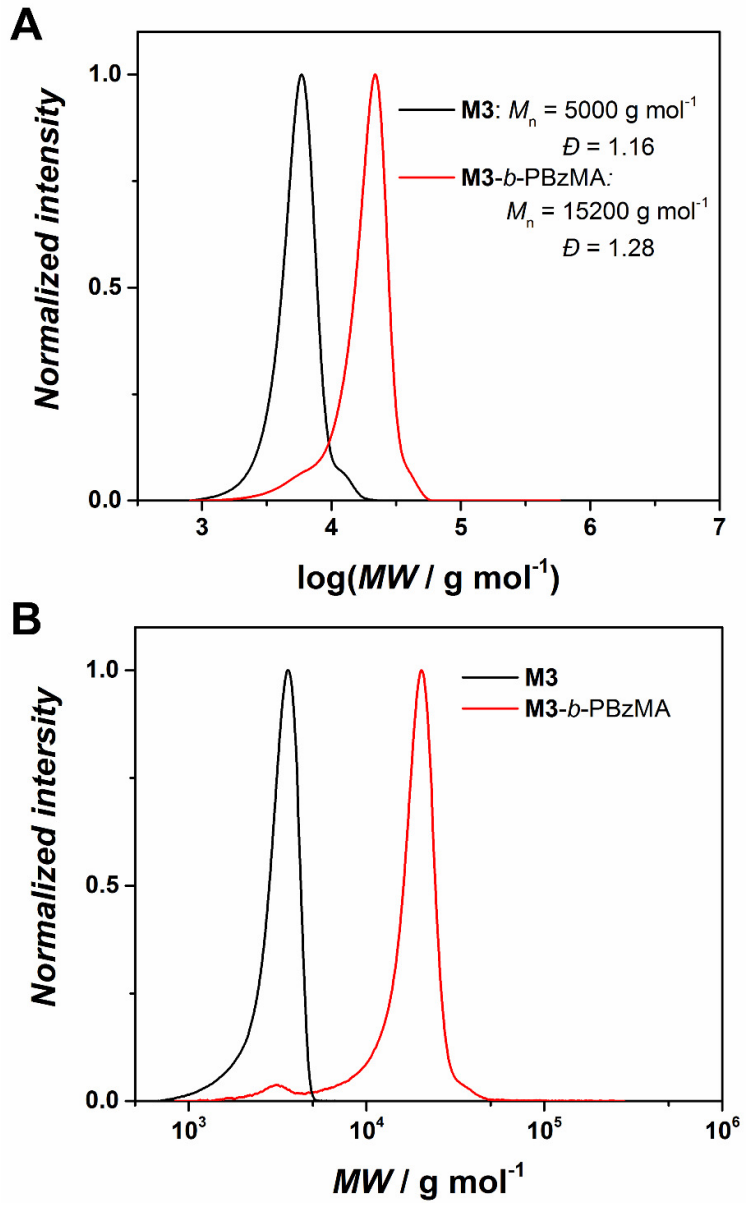

Figure S14. Size-exclusion chromatograms of **M3** and of its chain extension product with benzyl methacrylate in DMAc with RI detection (A) and in SEC with UV detection at 320 nm (B). *We note that in comparison to the use of a macroRAFT agent obtained by direct termination (see Figure S13), the fraction of non-chain extended PEtOx is considerably lower.*

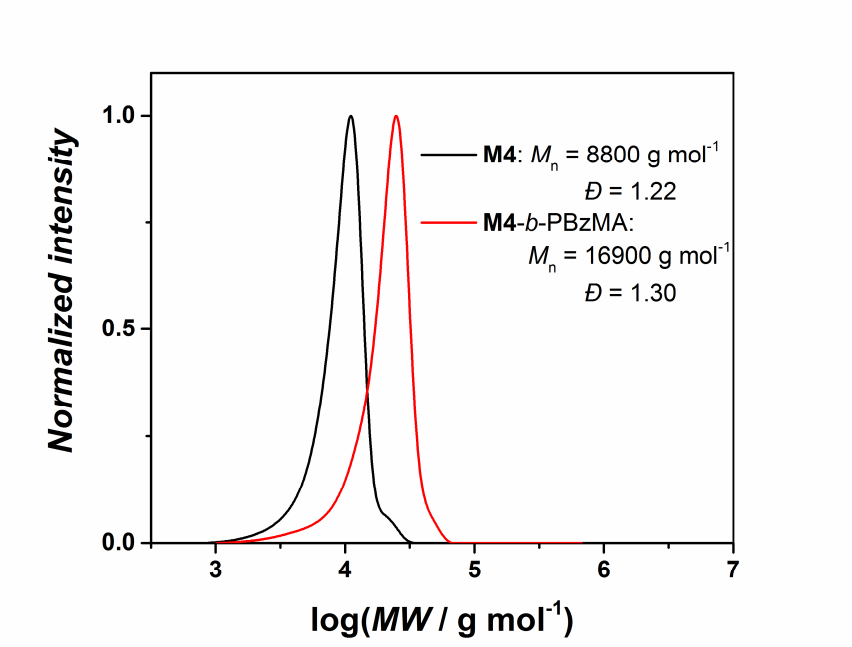

Figure S15. Size-exclusion chromatograms in DMAc of **M4** and of its chain extension product with benzyl methacrylate.

Polymerization-induced self-assembly (PISA) experiments

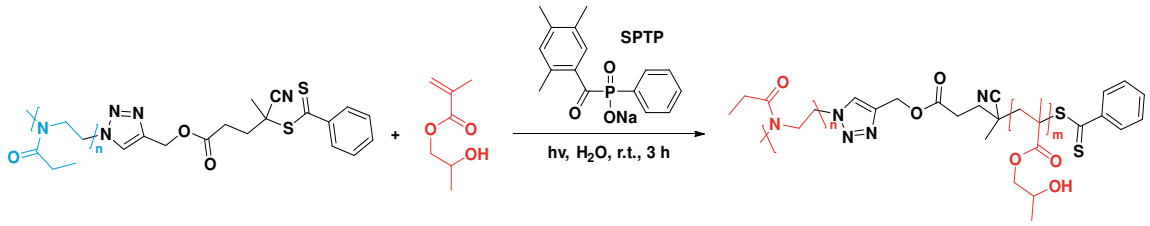

Poly(2-ethyl-2-oxazoline) macroRAFT agent **M1–4**, HPMA, SPTP, and water were added to a headspace vial with a stirring bar. The vials were closed air-tight and deoxygenated by nitrogen bubbling for 20 min. The polymerization mixtures were irradiated with a 23 W compact fluorescent lamp for 3 hours at room temperature in a homemade photoreactor. The reactor is built up of a cardboard covered with aluminum foil on the inside. The distance between the light source and the reaction tube is 20 cm.

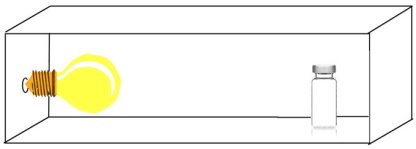

Scheme S1. Schematic reaction setup with a vial irradiated by a compact fluorescent lamp inside an aluminium foil-coated box for photoinduced RAFTPISA.

Table S3. Conditions and characterization results for polymers and nanoparticles synthesized by PISA in water using **M1** as macroCTA.

Entry	Structure	Total solids content / %	*Z-average*[a] nm	*PdI*[a]	$M_{n,SEC}$[b] g mol^{-1}	*Đ*[b]	Morphology[c]
1	**M1**-*b*-HPMA$_{30}$	5	40.7	0.166	9700	1.57	Sphere (S)
2	**M1**-*b*-HPMA$_{50}$	5	117.8	0.092	12700	1.76	S
3	**M1**-*b*-HPMA$_{75}$	5	141.3	0.042	17050	1.98	S
4	**M1**-*b*-HPMA$_{100}$	5	189.0	0.032	21500	1.89	S
5	**M1**-*b*-HPMA$_{30}$	10	40.7	0.146	9630	1.60	S
6	**M1**-*b*-HPMA$_{50}$	10	648.6	0.109	13100	1.69	S + Fibers (F)

Determined by [a]dynamic light scattering, [b]size-exclusion chromatography, and [c]transmission electron microscopy.

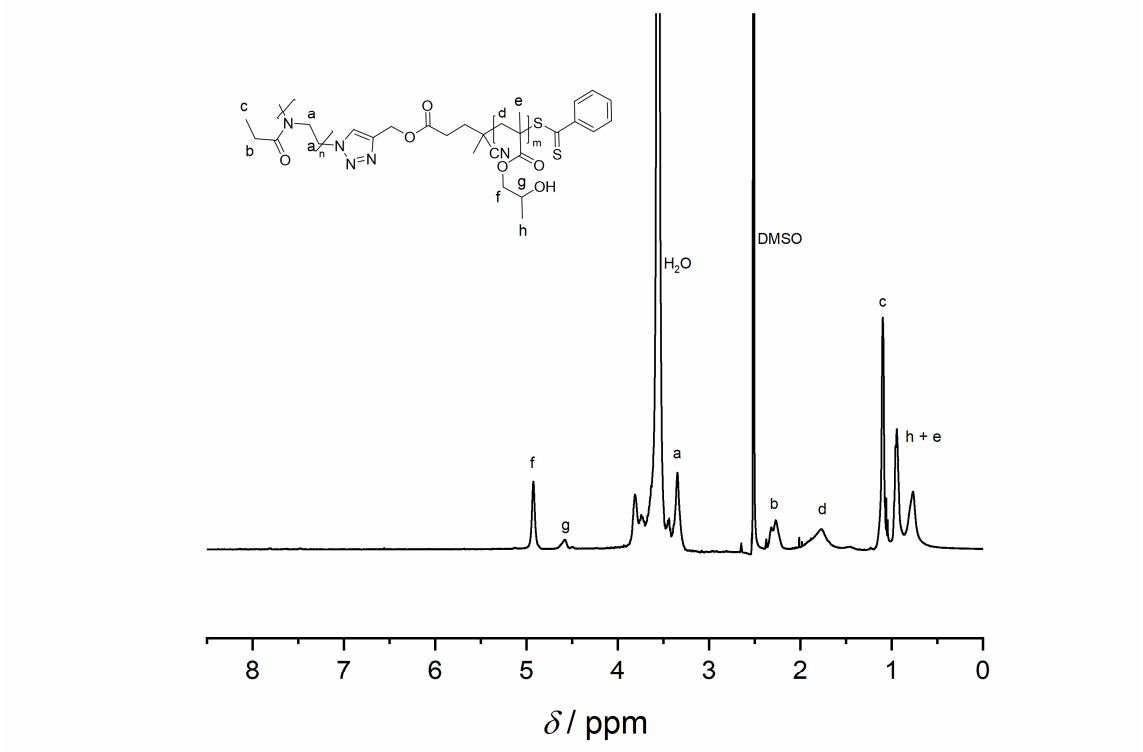

Figure S16. ^{1}H NMR spectrum of a non-purified PISA experiment mixture with **M1** after 3h (Entry 4, Table S2); solvent: DMSO-d_6.

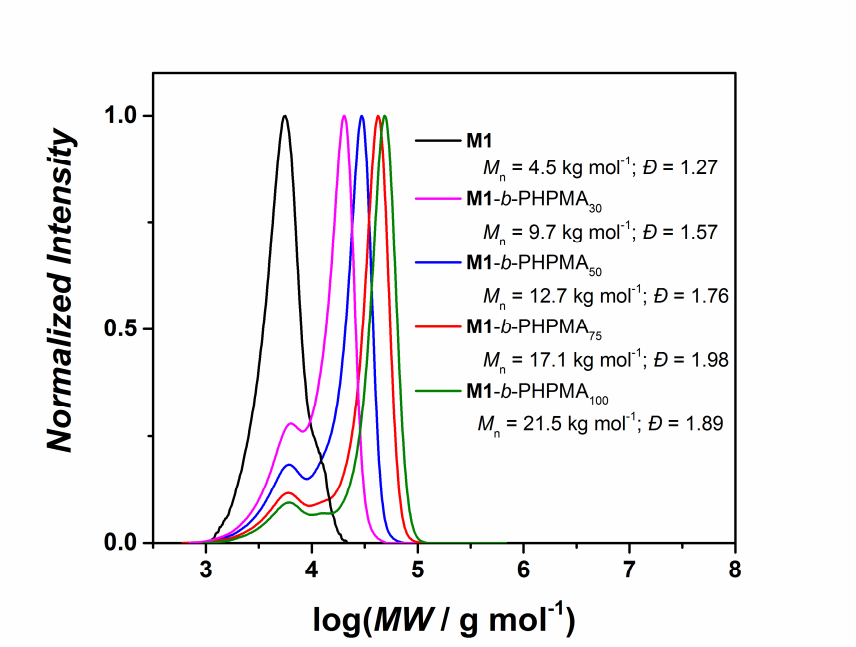

Figure S17. Size-exclusion chromatograms in DMAc of **M1** and corresponding block copolymers obtained by PISA with various DP_{HPMA} and with a total solids content of 5 wt%.

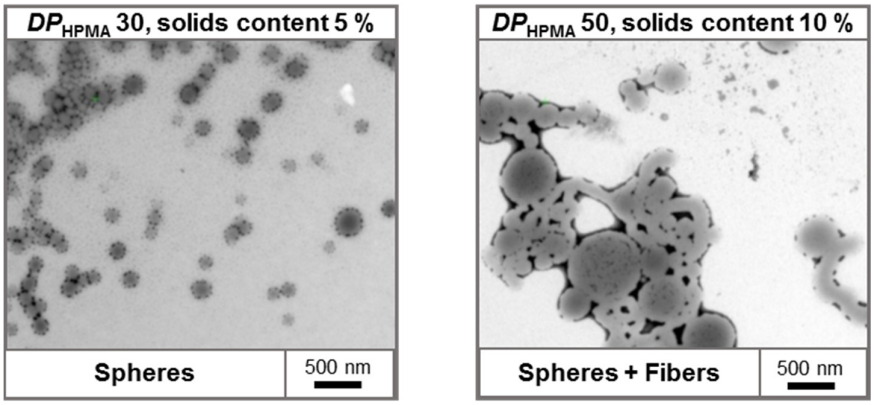

Figure S18. Representative TEM images of block copolymer NPs obtained by PISA with **M1**.

Table S4. Conditions and characterization results for polymers and nanoparticles synthesized by PISA in water using **M2** as macroCTA.

Entry	Structure	Total solids content / %	*Z-average*[a] nm	*PdI*[a]	$M_{n,SEC}$[b] g mol^{-1}	$Đ$[b]	Morphology[c]
1	**M2**-*b*-HPMA$_{50}$	5	27.9	0.155	14900	1.48	S
2	**M2**-*b*-HPMA$_{100}$	5	65.9	0.094	24500	1.63	S
3	**M2**-*b*-HPMA$_{150}$	5	71.6	0.100	25100	1.89	S
4	**M2**-*b*-HPMA$_{200}$	5	78.9	0.056	60400	1.11	S
5	**M2**-*b*-HPMA$_{50}$	10	31.1	0.247	18000	1.44	S
6	**M2**-*b*-HPMA$_{100}$	10	212.8	0.297	28700	1.34	S + F
7	**M2**-*b*-HPMA$_{150}$	10	170.5	0.130	32300	1.67	F + Vesicles (V)
8	**M2**-*b*-HPMA$_{200}$	10	179.0	0.095	34700	1.91	V
9	**M2**-*b*-HPMA$_{50}$	15	29.6	0.122	15800	1.55	S + F + V
10	**M2**-*b*-HPMA$_{100}$	15	1602	0.277	25400	1.63	F
11	**M2**-*b*-HPMA$_{150}$	15	1092	0.279	26500	1.82	V
12	**M2**-*b*-HPMA$_{200}$	15	685.9	0.173	40247	1.71	V

Determined by [a]dynamic light scattering, [b]size-exclusion chromatography, and [c]transmission electron microscopy.

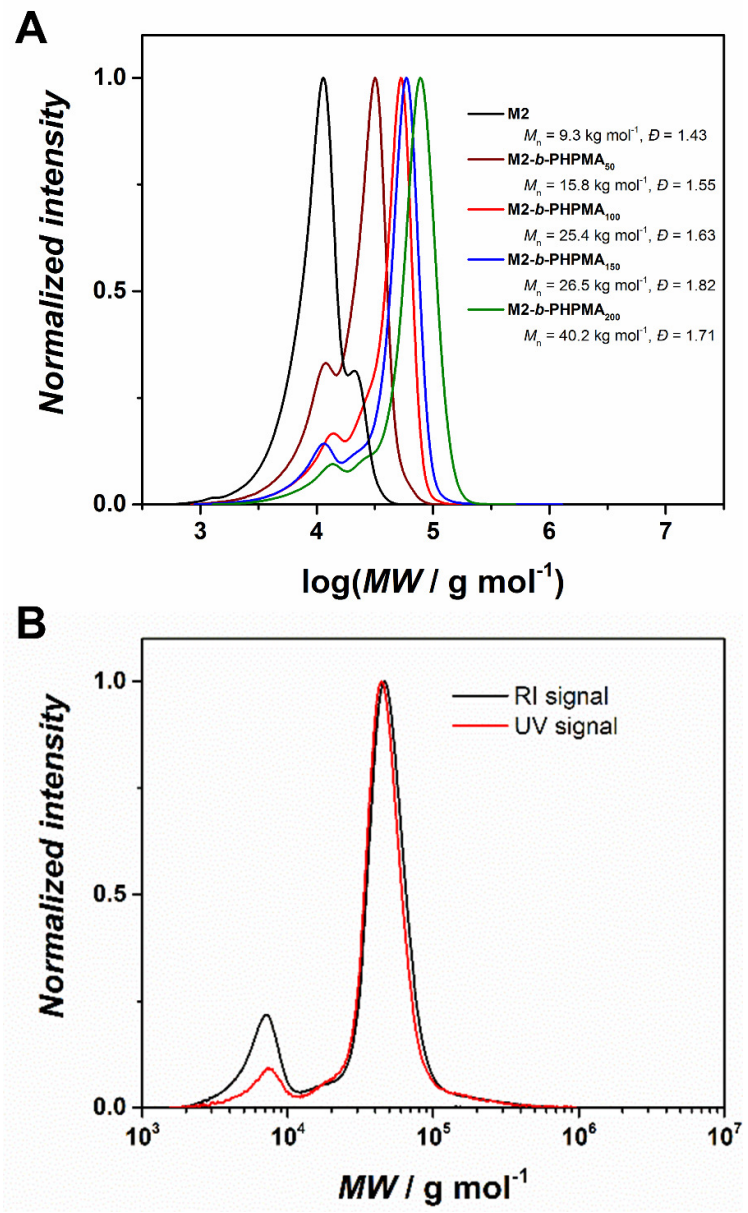

Figure S19. Size-exclusion chromatograms (A) in DMAc of **M2** and corresponding block copolymers obtained by PISA with various DP_{HPMA} and with total solids content of 15 wt% and (B) in THF of the PISA experiment carried out with **M2**, DP_{HPMA} of 200, and total solids content of 15 wt%. *Note that the UV signal stems mostly from the RAFT moiety, indicating here that the large majority of RAFT-capped PEtOx were chain-extended, yet that a small fraction were not.*

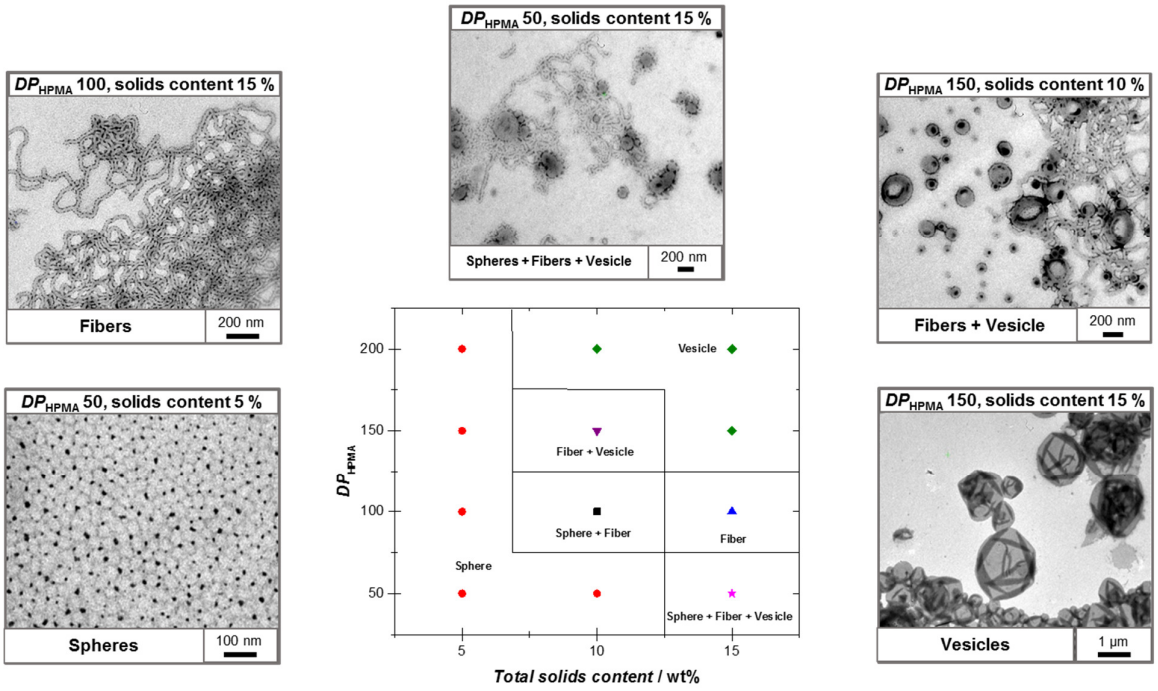

Figure S20. Phase diagram for nanoparticles synthesized by PISA in water using **M2** as macroCTA, along selected TEM images corresponding to these nanoparticles.

Table S5. Conditions and characterization results for polymers and nanoparticles synthesized by PISA in water using **M3** as macroCTA.

Entry	Structure	Total solids content / %	*Z-average*[a] / nm	*PdI*[a]	$M_{n,SEC}$[b] / g mol^{-1}	*Đ*[b]	Morphology[c]
1	**M3**-*b*-HPMA$_{50}$	5	27.7	0.162	12100	1.36	S
2	**M3**-*b*-HPMA$_{75}$	5	497.6	0.203	17600	1.32	S
3	**M3**-*b*-HPMA$_{100}$	5	227.5	0.151	21000	1.39	S
4	**M3**-*b*-HPMA$_{125}$	5	246.7	0.034	24700	1.46	S
5	**M3**-*b*-HPMA$_{150}$	5	227.5	0.041	28900	1.45	F
6	**M3**-*b*-HPMA$_{75}$	7.5	1254	0.271	18100	1.29	MNPs[d]
7	**M3**-*b*-HPMA$_{100}$	7.5	482.0	0.141	22500	1.28	S
8	**M3**-*b*-HPMA$_{150}$	7.5	505.9	0.020	24900	1.72	S
9	**M3**-*b*-HPMA$_{50}$	10	31.2	0.144	13600	1.29	S
10	**M3**-*b*-HPMA$_{60}$	10	59.0	0.166	15100	1.33	S
11	**M3**-*b*-HPMA$_{75}$	10	1329	0.127	17000	1.34	MNPs[d]
12	**M3**-*b*-HPMA$_{85}$	10	1241	0.084	19000	1.40	MNPs[d]
13	**M3**-*b*-HPMA$_{100}$	10	1057	0.027	20400	1.40	MNPs[d]

Determined by [a]dynamic light scattering, [b]size-exclusion chromatography, and [c]transmission electron microscopy. [d]Multicompartment nanoparticles.

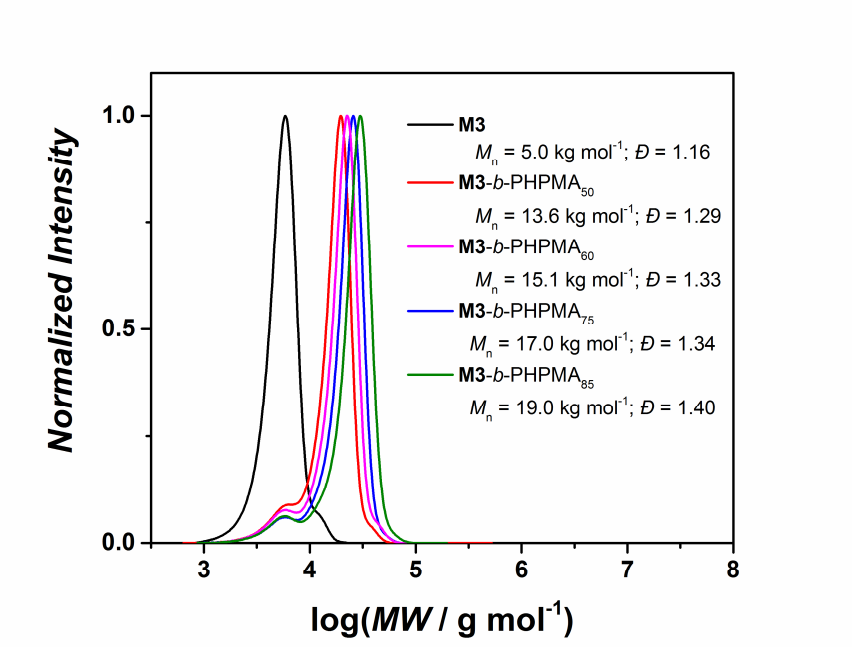

Figure S21. Size-exclusion chromatograms in DMAc of **M3** and corresponding block copolymers obtained by PISA with various DP_{HPMA} and with a total solids content of 10 wt%.

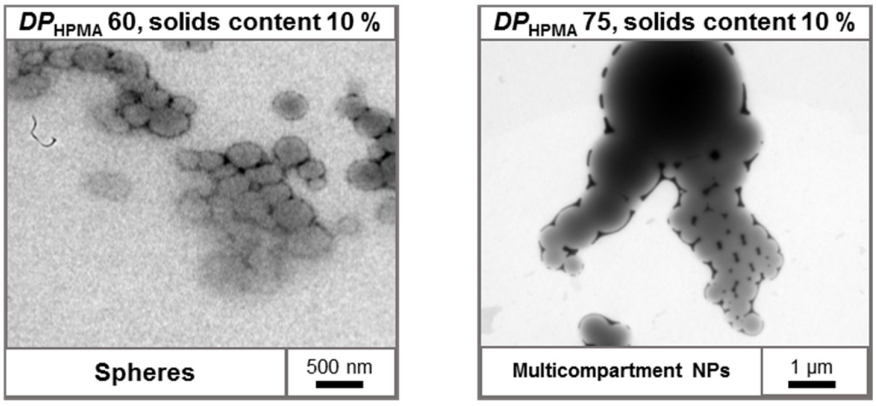

Figure S22. Representative TEM images of block copolymer NPs obtained by PISA with **M3**.

Table S6. Conditions and characterization results for polymers and nanoparticles synthesized by PISA in water using **M4** as macroCTA.

Entry	Structure	Total solids content / %	*Z-average*[a] nm	*PdI*[a]	$M_{n,SEC}$[b] g mol^{-1}	$Đ$[b]	Morphology[c]
1	**M4**-*b*-HPMA$_{50}$	5	95.1	0.627	13600	1.23	S
2	**M4**-*b*-HPMA$_{100}$	5	58.2	0.183	22000	1.40	S
3	**M4**-*b*-HPMA$_{150}$	5	81.1	0.172	26600	1.46	S
4	**M4**-*b*-HPMA$_{200}$	5	104.2	0.072	31300	1.53	Donut-like
5	**M4**-*b*-HPMA$_{50}$	10	28.7	0.329	14400	1.39	S
6	**M4**-*b*-HPMA$_{75}$	10	31.6	0.189	18300	1.38	S
7	**M4**-*b*-HPMA$_{100}$	10	45.1	0.196	23400	1.25	S
8	**M4**-*b*-HPMA$_{125}$	10	121.6	0.169	25800	1.35	S + F
9	**M4**-*b*-HPMA$_{150}$	10	1468	0.586	27900	1.41	Jellyfish-like (J)
10	**M4**-*b*-HPMA$_{175}$	10	1439	0.461	31300	1.36	J
11	**M4**-*b*-HPMA$_{200}$	10	1524	0.626	36200	1.41	V
12	**M4**-*b*-HPMA$_{50}$	15	26.4	0.325	13800	1.43	S
13	**M4**-*b*-HPMA$_{75}$	15	25.7	0.079	16600	1.42	S
14	**M4**-*b*-HPMA$_{100}$	15	30.8	0.116	19400	1.46	S
15	**M4**-*b*-HPMA$_{125}$	15	135.6	0.268	24300	1.43	F
16	**M4**-*b*-HPMA$_{135}$	15	105.4	0.144	25400	1.43	F
17	**M4**-*b*-HPMA$_{150}$	15	1331	0.080	29400	1.42	J
18	**M4**-*b*-HPMA$_{175}$	15	1226	0.276	34300	1.30	V
19	**M4**-*b*-HPMA$_{200}$	15	969.8	0.276	32300	1.45	V
20	**M4**-*b*-HPMA$_{50}$	20	25.7	0.299	13300	1.43	S
21	**M4**-*b*-HPMA$_{100}$	20	30.8	0.121	20400	1.41	S
22	**M4**-*b*-HPMA$_{125}$	20	76.7	0.158	26200	1.35	F
23	**M4**-*b*-HPMA$_{150}$	20	948.6	0.250	28900	1.39	J
24	**M4**-*b*-HPMA$_{200}$	20	11360	0.947	33204	1.42	precipitation

Determined by [a]dynamic light scattering, [b]size-exclusion chromatography, and [c]transmission electron microscopy.

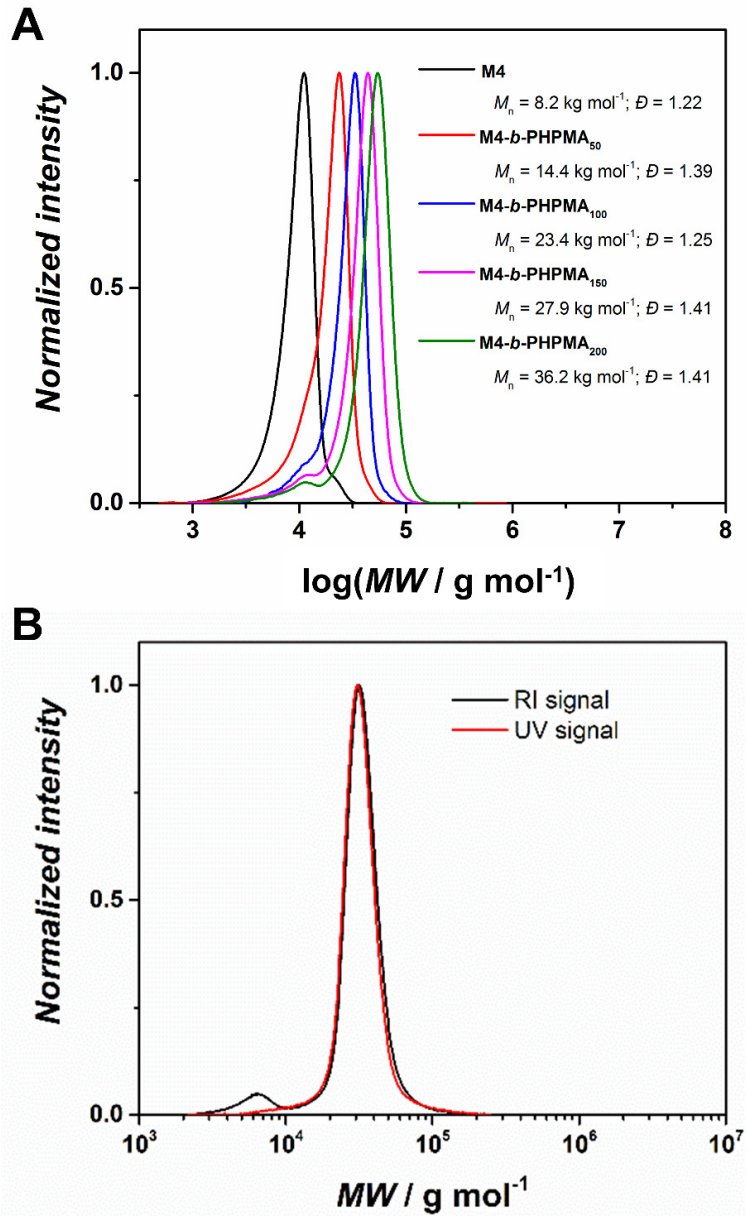

Figure S23. Size-exclusion chromatograms (A) in DMAc of **M4** and corresponding block copolymers obtained by PISA with various DP_{HPMA} and with a total solids content of 10 wt% and (B) of the PISA experiment carried out with **M4**, DP_{HPMA} of 200, and total solids content of 15 wt%. *Note that in contrast with PISA experiments carried out with **M2** (Figure S19), no residual macroRAFT agent is detected.*

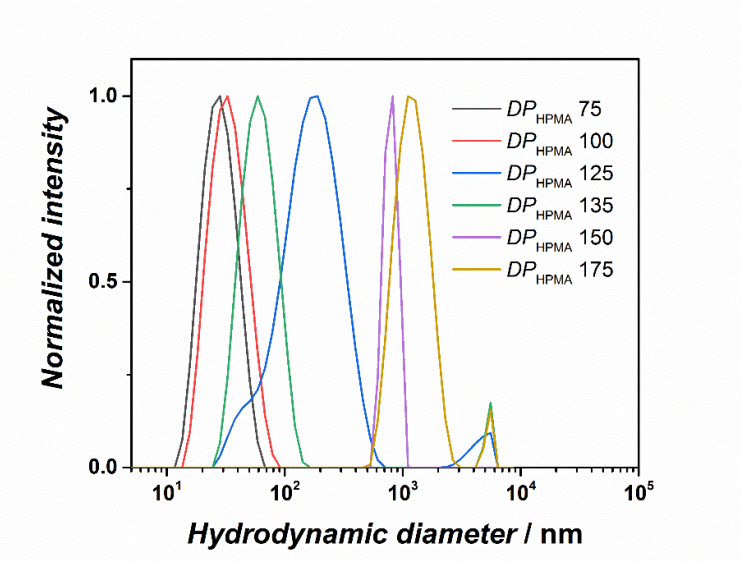

Figure S24. DLS results of NPs obtained by PISA of **M4** with various DP_{HPMA} and with a total solids content of 15 wt%.

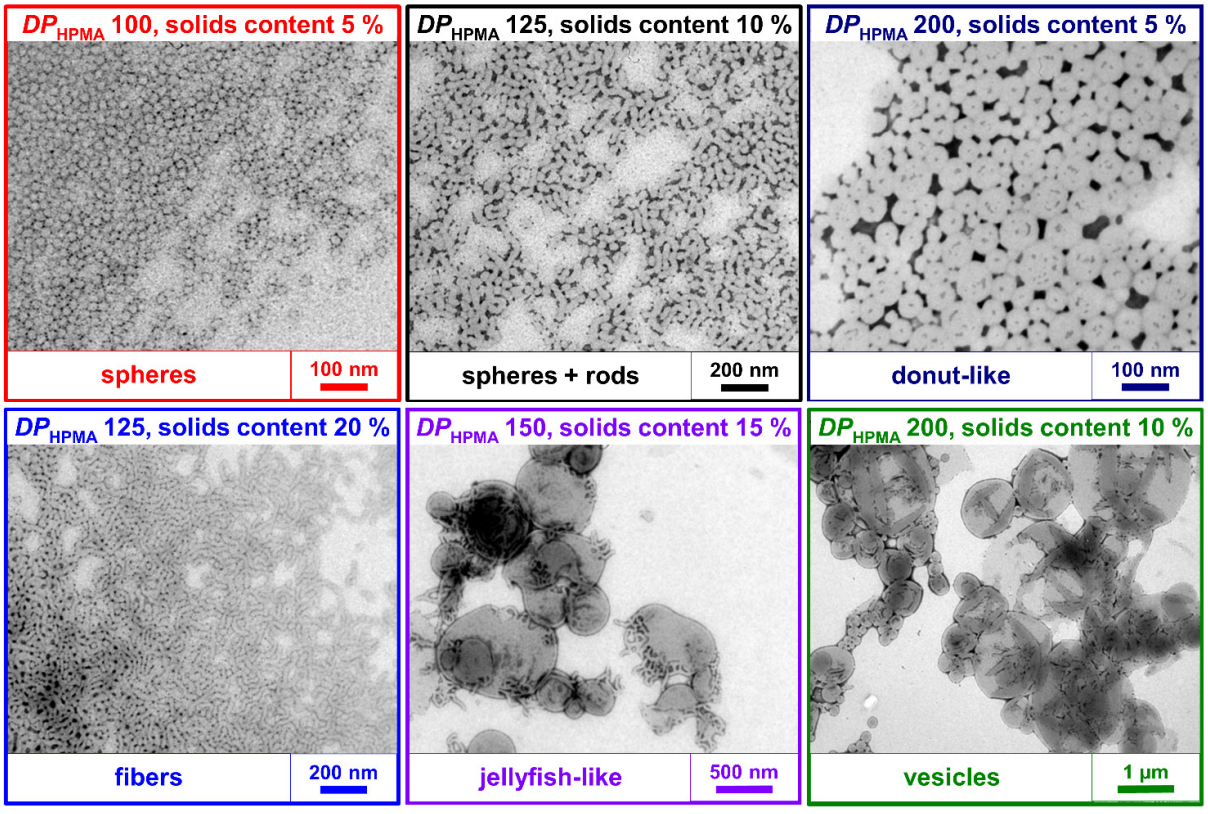

Figure S25. Enlarged TEM images presented in Figure 1.

Phase transition experiments

For high concentration solution: The solutions were kept at predetermined temperature for 4 h before dilution with water at the same temperature for TEM and DLS characterizations.

For low concentration solution: The solutions were kept at predetermined temperature for 24 h prior to DLS characterization.

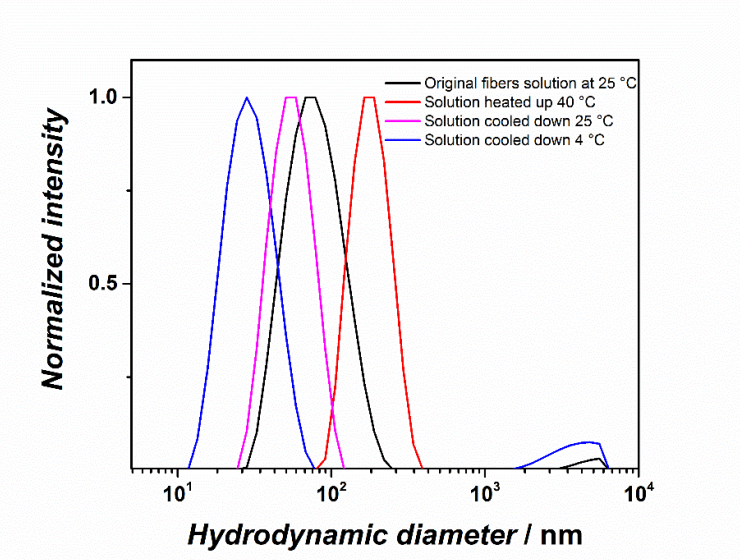

Figure S26. DLS results of original fiber solution (**M4**-*b*-PHPMA$_{125}$, 20 wt%, Table S6, Entry 22) at 25 °C in as-synthesized dispersion and at other temperature.

Synthesis of fluorescent PEtOx-based NPs

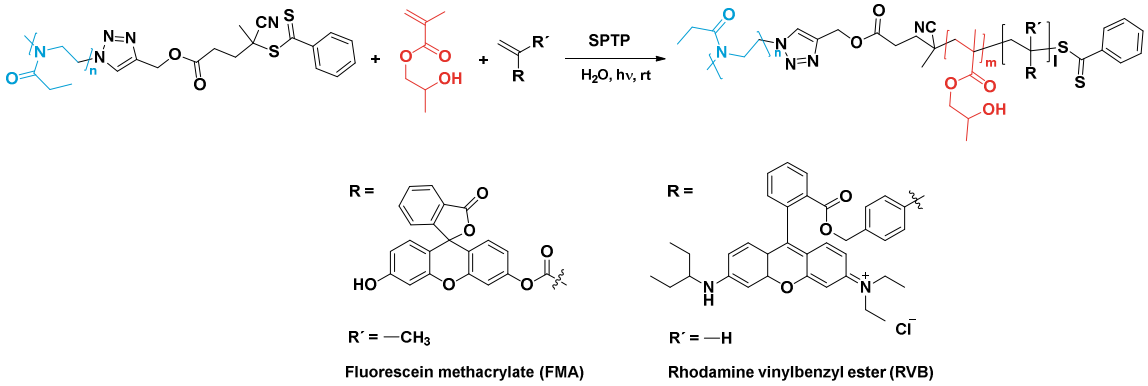

Scheme S2. Synthetic route towards fluorescein- or rhodamine-labeled nanoparticles by RAFTPISA utilizing PEtOx macroCTA.

Table S7. Characteristics of fluorescent NPs and constituting block copolymers.

Entry	Structure	*Z-average*[a] nm	*PdI*[a]	$M_{n,SEC}$[b] g mol^{-1}	*Đ*[b]	Morphology[c]
1	**M4**-*b*-(PHPMA$_{100}$-*co*-PFMA$_1$)	41	0.16	20100	1.42	S
2	**M4**-*b*-(PHPMA$_{100}$-*co*-PRVB$_{0.2}$)	60	0.12	18700	1.45	S

Determined by [a]dynamic light scattering, [b]size-exclusion chromatography, and [c]transmission electron microscopy.

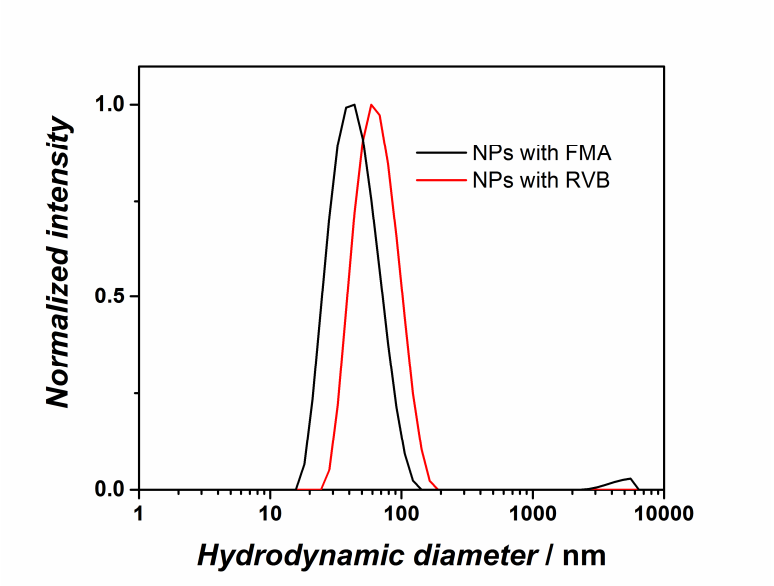

Figure S27. DLS results of fluorescent FMA-PEtOx NPs (black line) and RVB-PEtOx NPs (red line).

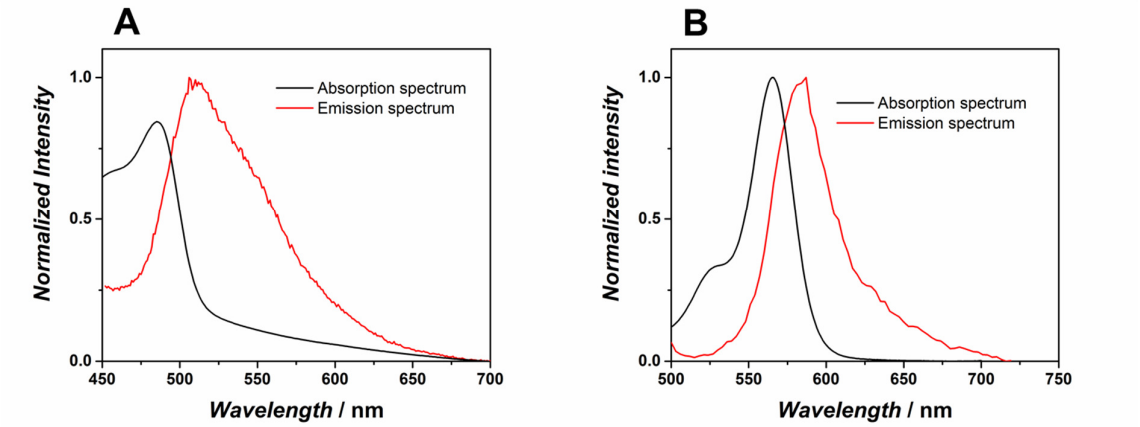

Figure S28. Absorption and emission spectra of (A) FMA-NPs (λ_{ex} = 490 nm) and (B) RVB-NPs (λ_{ex} = 555 nm).

Biological study – Experimental

All cells and zebrafish embryos were produced within our laboratories at the Institute of Toxicology and Genetics (ITG), affilitated to the Karlsruhe Institute of Technology (KIT), Karlsruhe, Germany.

Ethics statement
All zebrafish husbandry and experimental procedures were performed in accordance with the German and European animal protection standards and were approved by the Government of Baden-Württemberg, Regierungspräsidium Karlsruhe, Germany (AZ35-9185.81/G-137/10).

Zebrafish
Transgenic zebrafish (Danio rerio) Tg(kdrl.Hsa:HRAS-mCherry)s916/s896 and Tg(kdrl:EGFP)s843Tg were used. Fish were maintained at 28 °C as previously described.[3] Embryos at 3 dpf were used for the nanoparticle injection.

Preparation of nanoparticle dispersion for biological tests
For *in vitro* and *in vivo* studies, the stock solution of NPs was filtered through a 0.22 µm syringe filter for sterile filtration. Then, the solution was diluted to 100 µg mL^{-1} in DMEM 10% FBS or Medium 200/LSGS. The hydrodynamic diameters of NPs in diluted solutions were measured immediately (0 h) or after 24 h of incubation at 37 °C.

Intravenous injection of nanoparticles
Zebrafish embryos at 3 dpf were anaesthetized by 0.0168% w/v MS-222 (tricane methanesulfonate; Sigma-Aldrich) and embedded into 0.8% (w/v) low melting agarose with the right side of the embryo facing upward. Both, carboxylated polystyrene nanoparticles (PS-COOH NPs) and RVB-labeled PEtOx NPs were adjusted to 1.0 mg mL^{-1} (0.1% w/v solution) with distilled Milli-Q water (Millipore) containing 0.1% phenol red (P0290, Sigma-Aldrich) to visually assist the injection. Rhodamine-labeled Dextran was injected at equimolar concentration of the dye which was incorporated in the RVB-labeled PEtOx NPs. Prior to injection, the injection mix was sonicated in a water bath for 5 minutes to dissociate any agglomerates. A volume of 5 nL was injected into the common cardinal vein through a glass capillary connected with a FemtoJet microinjector (Eppendorf).

Confocal microscopy
A TCS SP5 confocal system with an upright configuration (DM6000; Leica Microsystems, Wetzlar, Germany) was used with a 63x water immersion objective (HCX APO L U-V-I 63.0x 0.90 WATER UV). For the detection of FITC-labelled PS NPs and GFP-labelled blood vessels, fluorescence was excited at 488 nm and detected in a range of 500-550 nm. RVB-labeled PEtOx NPs, rhodamine-conjugated dextran and mCherry fluorescence in the blood vessels were excited at 561 nm and detected through a window of 575-605 nm. PS NPs were labelled with green fluorescence and injected into *Tg(kdrl.Hsa:HRAS-mCherry)*$^{s916/s896}$. To minimize the read through between fluorescent channels, fluorescent images were acquired sequentially for each channel. The whole depth of the caudal vein region was scanned with z-interval of 1-2 µm and the whole length of caudal vein was imaged by tile scanning using a motorized stage.

Image analysis
Confocal and wide field fluorescent images were analysed with ImageJ/Fiji.[4]

Cell culture
Murine macrophages (RAW 264.7) were cultured in Dulbecco's Modified Eagle's Medium (DMEM) supplemented with 10% fetal bovine serum (FBS), 1% L-glutamine, and 1% penicillin/streptomycin. Human

lung epithelial carcinoma cells (A549) were cultured in DMEM medium supplemented with 10% FBS, 2mM L-glutamine, and 1% penicillin/streptomycin. Human umbilical vein endothelial cells (HUVEC) were cultured in Medium 200 supplemented with low serum growth supplement (LSGS) and 1% penicillin/streptomycin. All cell lines were cultivated at 37 °C, 5% CO_2 and with 95% relative humidity.

Cell viability determined by total cell number analysis

RAW 264.7 cells (1.25×10^4 cells/well), A549 cells (8×10^3 cells/well) and HUVECs (1×10^4 cells/well) were separately seeded in 96-well plates. After 18 h of attachment, cells were incubated with fluorescein-labeled PEtOx NPs at 25, 50, and 100 µg mL^{-1} for 24 h. Then, Hoechst 33342 (final concentration: 0.3 µg mL^{-1}) was added and incubated for 30 min at 37 °C and 5% CO_2. Finally, four images per well were acquired using the automated fluorescence microscope IX81 (Olympus, Germany) with a 10-fold objective and DAPI cubic filters. Automated image analysis was carried out using the Olympus ScanR analysis software as previously described.[5] The total number of cells was determined by counting the Hoechst-stained nuclei. Cell viability was expressed by (cell number in treatment group)/(cell number of unexposed control) × 100. Mean values ± SEM are given from two independent experiments.

Cellular uptake and quantification

All steps were the same as mentioned above. After Hoechst staining for 30 min, all medium was discarded and 100 µL fresh medium was added. NP uptake was detected by automated fluorescence microscopy employing GFP (ex. 457–487 nm; em. 502–538 nm) cubic filters (Olympus IX81, Olympus Corporation, Japan) with a 20-fold objective. Images were collected at exposure times of 4 ms, 50 ms, and 500 ms. The morphology of cells and outline of nuclei were also detected in the bright-field and DAPI channel, respectively. To quantify the cellular uptake, the total fluorescence intensity detected in the GFP channel was analyzed by the ScanR software. The total number of cells per image were obtained by enumerating all nuclei as identified by edge detection in the DAPI channel. The mean fluorescence intensity per cell (MFI/cell) could be calculated with the following equation:

$$\text{MFI/cell} = (\text{total fluorescence})/(\text{total cell number})$$

Around 1000 RAW, 500 A549, and 150 HUVEC cells were analyzed per treatment and the average cellular uptake (MFI/cell) was quantified. The brightness of FMA-labeled PEtOX NPs and PS-COOH NPs in water at 100 µg mL^{-1} was measured at wavelengths of 485 ± 10 nm for excitation and 530 ± 13 nm for emission using a fluorescence reader (MWG-Biotech AG, Ebersberg, Germany). The fluorescence intensity of PS-COOH NPs is about 9.5 times higher than that of FMA-labeled PEtOx NPs. Thus, when quantifying the mean fluorescence intensity per cell, the intensity of PEtOx NPs was multiplied by 9.5 to compensate for the intensity differences between the two types of particles.

Statistics

A two-tailed student's t-test was used to compare significant differences between control and treatment groups.

Biological studies – Detailed *in vitro* results and extended discussion

Particle size and stability in relevant biological media

Table S8. Hydrodynamic diameters obtained by DLS for FMA-PEtOx NPs and PS-COOH nanoparticles in water and cell culture media.

	FMA-PEtOx NPs			PS-COOH NPs		
	Z-av.[b]	*PdI*[c]	D_n[d]	*Z-av.*[b]	*PdI*[c]	D_n[d]
Water (0 h)	41.5	0.16	21	113.5±0.7[a]	0.03[a]	91.3[a]
DMEM/FCS (0 h)	43.8±0.5	0.28	4.8	173.8±2.3	0.12	105.7
DMEM/FCS (24 h)	186.1±2.8	0.15	105.7	155.6±4.6	0.10	91.3
M200/LSGS (0 h)	40.5±0.6	0.16	18.2	315.6±33.2	0.22	122.4
M200/LSGS (24 h)	152.9±0.4	0.08	105.7	1291±309	0.56	105.7

[a]Data was derived from our previous study.[5] [b]*Z-average* (*Z-av.*) is an intensity-based mean hydrodynamic diameter obtained by NanoZS system. The main peak (Peak 1) was used to express the mean intensity-based diameter for all cell culture media to avoid interferences due to small-sized serum proteins. [c]*PdI* = polydispersity as obtained with the NanoZS system (0 < *PdI* < 1) reflects the breadth of the particle hydrodynamic diameter distribution. [d]D_n= number-based peak intensity as obtained with NanoZS system.

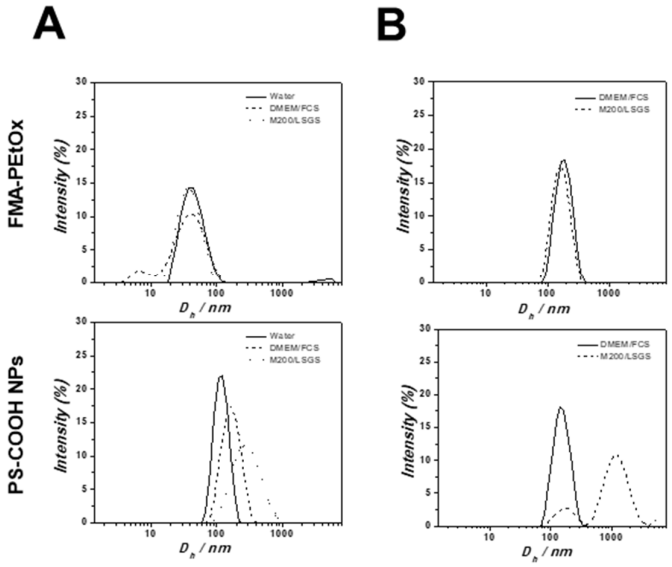

Figure S29. Intensity-based hydrodynamic diameter distributions of FMA-labeled PEtOx NPs and PS-COOH NPs in water and cell culture media (DMEM/FCS and M200/LSGS) at 0 h (A) and 24 h (B).

Fluorescence intensity of the fluorescein-labeled PEtOx nanoparticles

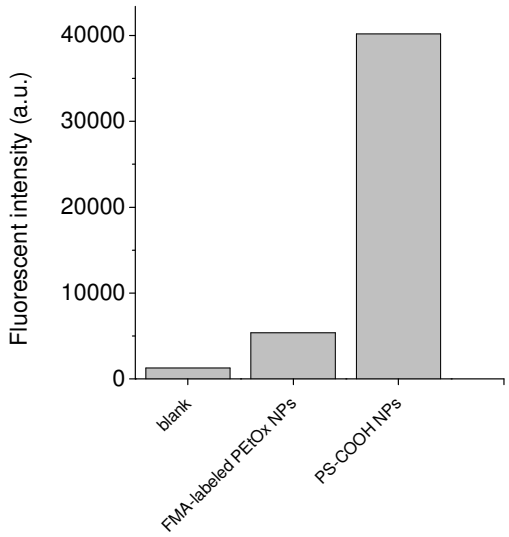

Figure S30. Fluorescence intensities of FMA-labeled PEtOx NPs and PS-COOH NPs in water at 100 µg mL^{-1}. This data was collected with a fluorometer under excitation wavelength 485 ± 10 nm and emission wavelength 530 ± 13 nm.

Assessment of cellular uptake and viability in vitro

To evaluate the potential of NPs being as biomedical devices, it is crucial to firstly assure biocompatibility and the ability to evade clearance by the reticuloendothelial system (RES). When NPs are injected into the blood stream, they generally are recognized and removed by macrophages or endothelial cells, leading to a low targeting ratio.[6–10] Carboxylated polystyrene (PS-COOH), a common commercial polymeric NP, has been investigated with respect to biocompatibility and uptake by macrophages and endothelial cells.[11] Therefore, it is suited as reference material for comparison. Three representative mammalian cell types were used here: phagocytic cells (murine macrophages RAW 264.7), endothelial cells (human umbilical vein endothelial cells; HUVECs), and epithelial cells (human lung epithelial carcinoma A549 cells).

In the uptake study, no accumulation of PEtOx NPs could be found in all cell types and at all tested concentrations after 24 h of incubation (Figures S31–S33; A). However, PS-COOH NPs could be detected to some extent in A549 cells and more pronounced in RAW 264.7 cells and HUVECs. Quantitative data derived for the experiments with FMA-labeled PEtOx NPs also showed significantly lower average fluorescence intensities per cell than after incubation of cells with PS-COOH NPs (Figures S31–S33; B). Please note that the intensity in PEtOx NPs groups was multiplied by a factor of 9.5 because of the difference in fluorescence intensity (as described above) at the same concentration (Figure S30). Upon increasing the charge-coupled device exposure time (i.e., 50 or 500 ms), a few bright dots could be observed which, however, were not associated with cells. This might be due to slight aggregation of PEtOx NPs in the two cell culture media after 24 h of incubation, i.e., DMEM/FCS and M200/LSGS (Table S7 and Figure S29). Concerning the biocompatibility, cell viability in the presence of PEtOx NPs did not change significantly in the three cell types (Figures S31–S33; C), while reduced cell viability was found in A549 and RAW264.7 cells after exposure to PS-COOH NPs.

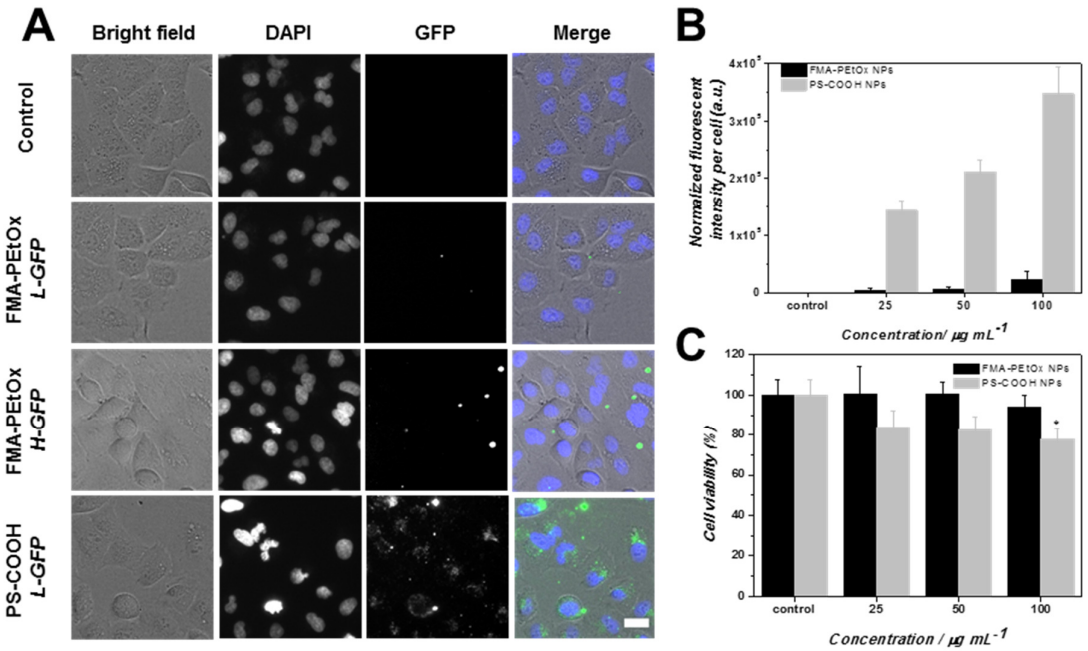

Figure S31. Cytotoxicity and cellular uptake of NPs in A549 cells. (A) Cellular uptake of FMA-PEtOx NPs and PS-COOH upon 24 h exposure of cells (100 µg/mL). GFP signal was captured by automated fluorescence microscopy at either 50 ms (L-GFP, L: low) or 500 ms (H-GFP, H: high) exposure time. Scale bar= 20 µm. (B) Quantitative uptake analysis depicted as average total fluorescence intensities (all using 50 ms exposure time). For an appropriate comparison, the fluorescence intensity per cells after exposure to the FMA-PEtOx NPs were multiplied by a factor of 9.5 because of the intrinsic intensity differences between FMA-PEtOx and PS-COOH NPs. Values are represented as mean ± SD. (C) Cytotoxicity of NPs. Data are representative for 2 independent experiments each performed in triplicates and shown as means ± SEM. (*) Significantly different from control group (*$p<0.05$, **$p<0.01$).

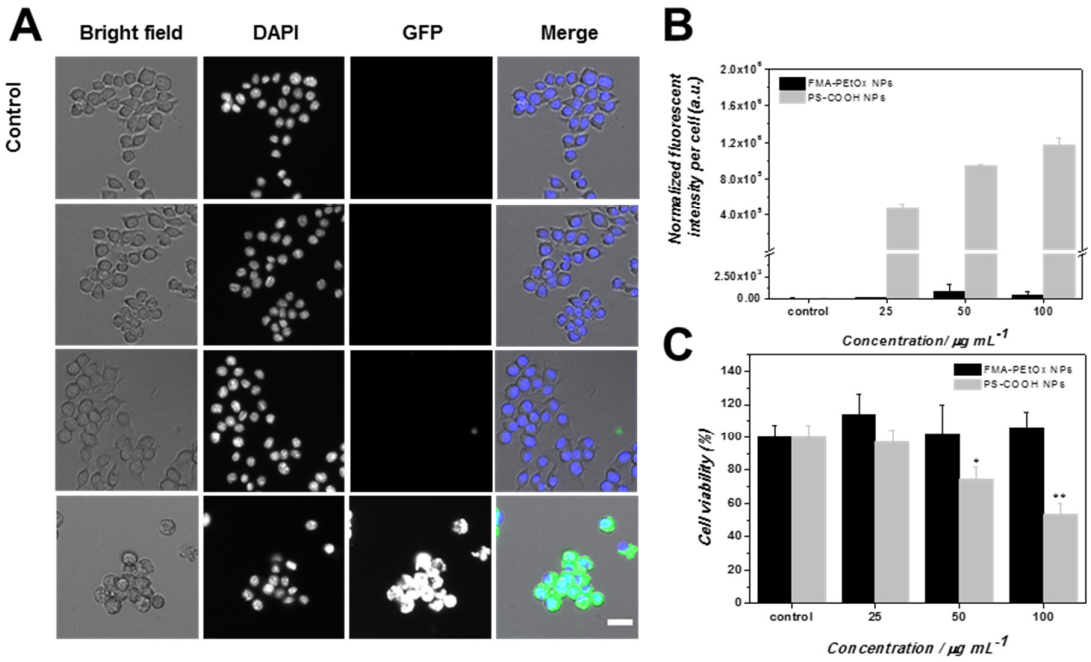

Figure S32. Cytotoxicity and cellular uptake of NPs in RAW264.7 cells. (A) Cellular uptake of FMA-PEtOx NPs and PS-COOH upon 24 h exposure of cells (100 µg/mL). GFP signal was captured by automated fluorescence microscopy at either 4 ms (L-GFP) or 50 ms (H-GFP) exposure time. Scale bar= 20 µm. (B) Quantitative uptake analysis were performed as described in Fig S30 (all at 4 ms exposure time). (C) Cytotoxicity of NPs. Data are representative for 2 independent experiments each performed in triplicates and shown as means ± SEM. (*) Significantly different from control group (*p<0.05, **p<0.01).

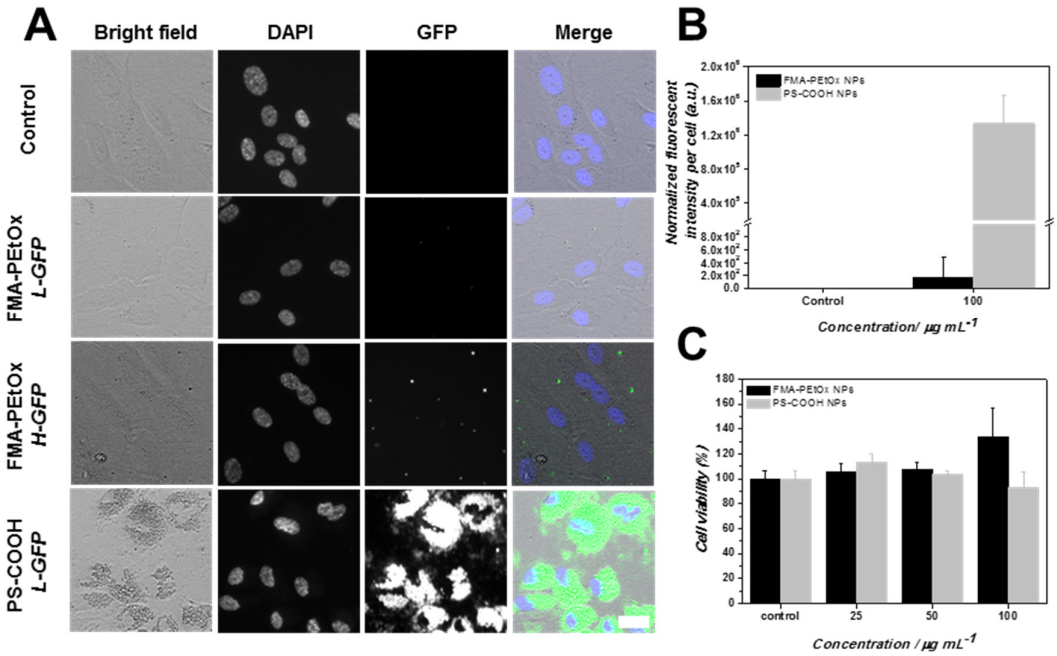

Figure S33. Cytotoxicity and cellular uptake of NPs in HUVEC cells. For details see Fig. S31.

Biodistribution and compatibility of NPs in zebrafish embryos

For the application of NPs for drug delivery, it is crucial that NPs escape clearance by the reticuloendothelial system (RES). The caudal vein (CV) of the zebrafish embryo was used as a model to assess how NPs interact with endothelial cells and macrophages.[5,12]. To this end, we systemically administered PEtOx NPs by injecting them into the common cardinal vein of 3 dpf embryo and examined their biodistribution at 24 hours-post-injection (hpi). To visualize blood vessels, Tg(kdrl.Hsa:HRAS-mChe)s896Tg or Tg(kdrl:EGFP)s843Tg transgenic zebrafish embryos were used. In addition to PS-COOH NPs, which lack stealth properties and hence are entrapped in the RES[5] also rhodamine-conjugated 3 kDa dextran was used as another positive control. Rhodamine-conjugated 3 kDa dextran (6.1 µM; 0.5-1.0 rhodamine per dextran molecule) were injected at equimolar concentration of rhodamine as incorporated in 1 mg mL^{-1} PEtOx NPs to assess a possible release of the rhodamine fluorophore from NPs and/or disassembling of NPs into polymer chains. Indeed, opposed to the behavior of rhodamine-conjugated dextran, which accumulated to a minor extent in endothelial cells and was rapidly cleared, PEtOx NPs mainly circulated in the bloodstream and were also taken up by macrophages. The clear difference in the biodistribution of the fluorophore when either coupled to dextran or incorporated into NPs indicates no major release of the fluorophore from NPs *in vivo*.

References

1 J. Tong, Y. Shi, G. Liu, T. Huang, N. Xu, Z. Zhu and Y. Cai, *Macromol. Rapid Commun.*, 2013, **34**, 1827–1832.

2 J.-F. Lutz, S. Pfeifer, M. Chanana, A. F. Thünemann and R. Bienert, *Langmuir*, 2006, **22**, 7411–7415.

3 M. Westerfield, *The Zebrafish Book: A Guide for the Laboratory Use of Zebrafish (Danio Rerio)*, Institute of Neuroscience. University of Oregon, 2000.

4 J. Schindelin, I. Arganda-Carreras, E. Frise, V. Kaynig, M. Longair, T. Pietzsch, S. Preibisch, C. Rueden, S. Saalfeld, B. Schmid, J. Y. Tinevez, D. J. White, V. Hartenstein, K. Eliceiri, P. Tomancak and A. Cardona, *Nat. Methods*, 2012, **9**, 676–682.

5 S. R. Mane, I. L. Hsiao, M. Takamiya, D. Le, U. Straehle, C. Barner-Kowollik, C. Weiss and G. Delaittre, *Small*, 2018, **14**, 1801571.

6 S. Wilhelm, A. J. Tavares, Q. Dai, S. Ohta, J. Audet, H. F. Dvorak and W. C. W. Chan, *Nat. Rev. Mater.*, 2016, **1**, 16014.

7 J. Davda and V. Labhasetwar, *Int. J. Pharm.*, 2002, **233**, 51–59.

8 C. Freese, D. Schreiner, L. Anspach, C. Bantz, M. Maskos, R. E. Unger and C. J. Kirkpatrick, *Part. Fibre Toxicol.*, 2014, **11**, 68.

9 S. M. Moghimi, A. C. Hunter and J. C. Murray, *FASEB J.*, 2005, **19**, 311–330.

10 M. I. Setyawati, C. Y. Tay, D. Docter, R. H. Stauber and D. T. Leong, *Chem. Soc. Rev.*, 2015, **44**, 8174–8199.

11 O. Lunov, T. Syrovets, C. Loos, J. Beil, M. Delacher, K. Tron, G. U. Nienhaus, A. Musyanovych, V. Mailänder, K. Landfester and T. Simmet, *ACS Nano*, 2011, **5**, 1657–1669.

12 F. Campbell, F. L. Bos, S. Sieber, G. Arias-Alpizar, B. E. Koch, J. Huwyler, A. Kros and J. Bussmann, *ACS Nano*, 2018, **12**, 2138–2150.